Departement für Pferde, Klinik für Pferdechirurgie
der Vetsuisse-Fakultät Universität Zürich

Vorsteher Departement für Pferde:
Prof. Dr. med. vet. Colin Schwarzwald, PhD, Dipl. ACVIM / ECEIM

Direktor Klinik für Pferdechirurgie:
Prof. Dr. med. vet. Anton Fürst, Dipl. ECVS

Musculoskeletal Research Unit (MSRU)
Leiterin: Prof. Dr. med. vet. Brigitte von Rechenberg, Dipl. ECVS

Arbeit unter wissenschaftlicher Betreuung von Salim Elias Darwiche, PhD

Tracking Cells in Osteochondral Explants: A study on Cartilage Remodeling

Inaugural-Dissertation

zur Erlangung der Doktorwürde
der Vetsuisse-Fakultät Universität Zürich

vorgelegt von

Serah Naomi Saitowitz

Tierärztin
aus Mörlenbach im Odenwald, Deutschland

genehmigt auf Antrag von

Prof. Dr. med. vet. Brigitte von Rechenberg, Referentin

Prof. Dr. sc. nat. Cornel Fraefel, Korreferent

2018

Departement für Pferde, Klinik für Pferdechirurgie
der Vetsuisse-Fakultät Universität Zürich

Vorsteher Departement für Pferde:
Prof. Dr. med. vet. Colin Schwarzwald, PhD, Dipl. ACVIM / ECEIM

Direktor Klinik für Pferdechirurgie:
Prof. Dr. med. vet. Anton Fürst, Dipl. ECVS

Musculoskeletal Research Unit (MSRU)
Leiterin: Prof. Dr. med. vet. Brigitte von Rechenberg, Dipl. ECVS

Arbeit unter wissenschaftlicher Betreuung von Salim Elias Darwiche, PhD

Tracking Cells in Osteochondral Explants: A study on Cartilage Remodeling

Inaugural-Dissertation

zur Erlangung der Doktorwürde
der Vetsuisse-Fakultät Universität Zürich

vorgelegt von

Serah Naomi Saitowitz

Tierärztin
aus Mörlenbach im Odenwald, Deutschland

genehmigt auf Antrag von

Prof. Dr. med. vet. Brigitte von Rechenberg, Referentin

Prof. Dr. sc. nat. Cornel Fraefel, Korreferent

2018

The heights by great *wo*men reached and kept, were not attained by sudden flight, but they, while their companions slept, were toiling upward in the night.

With lots of love and profound gratitude to
my loving parents Brian and Beate
and my wonderful sister Shoshana.
&
In fondest memory of the most inspiring veterinarian
Dr.med.vet. Josef Michael Emil Wolfschaffner
**** 27.11.1953 † 24.12.2010***

Zusammenfassung

Das kaum erforschte Gebiet der Knorpelremodellierung wurde in dieser Dissertation noch einmal genauer untersucht. Jahrelang wurde angenommen, Gelenkknorpel und fetaler Wachstumsfugenknorpel würden gleichermassen agieren, was bedeutet, dass Knorpelzellen in der kalzifizierten Zone des Gelenkknorpels hypertroph und apoptotisch sind. Auch ein physiologischer Remodellierungsprozess des intakten Knorpelgewebes durch Zellen aus dem subchondralen Knochen wurde nicht für möglich gehalten. Allzu oft wurde Knochen und Knorpel separat betrachtet, obwohl sie denselben embryonalen Ursprung haben.

Ziel dieser Arbeit war es, die Vitalität und Migrationsfähigkeiten von Zellen aus dem subchondralen Knochen in den darüber liegenden hyalinen Gelenksknorpel zu beobachten. Mit Hilfe einer osteochondralen Explantatkultur gelang es mit speziellen Lebendfärbungen, die unter anderem auch Veränderungen des Aktinskeletts deutlich machten, die einzelnen Zellen über einen definierten Zeitraum mittels Zeitraffer in einem CLSM (Confocal Laser Scanning Microscope) darzustellen und zu verfolgen. Die Migration der Zellen konnte im physiologischen sowie im pathophysiologischen Zustand mit, bzw. ohne Einwirkung von Entzündungsfaktoren, in vitro demonstriert werden.

Dies beweist, dass subchondraler Knochen und Gelenkknorpel als Einheit betrachtet werden sollten und dass eine Remodellierung in diesem Gewebe durchaus möglich ist.

Summary

The scarcely researched field of cartilage remodeling was examined in detail in this thesis. For years, it was thought that cartilage in joints behaves the same way as cartilage of the growth plate, which means that cells in the calcified zone of articular cartilage are hypertrophic and apoptotic. Also, a physiological remodeling process of the intact cartilaginous tissue, through cells from the subchondral bone, was not considered possible. Often bone and cartilage are contemplated separately, although they have the same embryonic origin.

The aim of this work was to check on the viability of cells and to detect migration of cells from the subchondral bone into the overlying hyaline articular cartilage by developing a method to image labelled cells within cultured osteochondral explants.

By using an osteochondral explant culture, the individual cells could be supervised and tracked in a CLSM (Confocal Laser Scanning Microscope) over a certain time period (time-lapse recording) using special live protein stains, which also showed changes in the actin skeleton. The migration of the cells was shown in vitro in homeostasis as well as in pathophysiological state, with and without the influence of inflammatory factors.

This proves that subchondral bone and articular cartilage should be viewed as a unit and that a remodeling in this tissue is possible.

1 Introduction

1.1 Purpose of dissertation

Remodeling means breaking down existing tissue and rebuilding it, either as a tissue of similar or even better value. In case of repair, the broken-down tissue is replaced with tissue of minor quality. This process does not only take place as a result of damage, but also takes place during homeostasis, to keep the tissue intact and maintain it.

Most tissues in the body have the ability to remodel, except for articular hyaline cartilage, where this was never demonstrated. This fact makes one wonder why this is not supposed to also be the case in articular cartilage. Inflammation, granulation, reparation and remodeling are the basic phases of healing in the body. One would assume that this should also be possible in cartilage.

The greatest difference in comparison to all other tissues is, that articular cartilage is free of blood vessels and a-lymphatic. How do molecules manage to get where they are needed, without blood? Along that line, the physiological remodeling mechanisms of the articular hyaline cartilage matrix over time is also still not clearly understood, although enzymes degrading the matrix have been identified. Additionally, there is no clarity about the life expectancy of cartilage cells, so-called chondrocytes, and/or whether chondrocytes can migrate or stay at their set location within the matrix throughout their viable phase.

It also is not fully understood yet, which physiological mechanisms – or molecular cross talks are ongoing between subchondral bone and articular hyaline cartilage. In fact, there is a common belief, that subchondral bone and overlying cartilage are separate structures in adult life, although we know the connections between these during fetal development and during growth of the skeleton post-partum. This assumption is questioned in this study, since biologically this complete separation in adult life does not make real sense. It starts with the fact, that cells are commonly observed within the calcified cartilage zone in normal cartilage. In addition, “cutting cones” reaching from the subchondral bone into the calcified cartilage zone, similar to the ones in bone remodeling, are commonly visualized in healthy and osteoarthritic cartilage. Therefore, it is of enormous importance to study subchondral bone and the hyaline cartilage as a biological unit, also on behalf of the remodeling process. If the subchondral bone is damaged, for example, it will always also cause a breakdown of the overlying cartilage. The other way around a cartilage defect also always causes a change in subchondral bone[2-4]. This makes sense, also due to the fact

that subchondral bone is provided with vasculature that is thought to nourish also the deepest zones of the cartilage through diffusion. Besides the molecules coming from the synovia, that reach the cartilage through diffusion and load, it seems like the only other way of receiving information or signals is from the subchondral bone. Still, there must be a chance for cartilage to remodel from either the cartilage-side and/or the subchondral bone plate. Possibly, progenitor cells make their way through subchondral bone into the cartilage as this occurs in full cartilage lesions. Possibly, it could also be that these cells differentiate into mature chondrocytes and migrate further within the extracellular matrix? And if so, which factors cause and/or accelerate this process? Looking at cytokines causing osteoarthritis, it could well be that these or similar factors could initiate a migration process of the progenitor cells, respectively chondrocytes in articular cartilage from either the subchondral bone to cartilage or from the cartilage surface towards the deeper matrix or even to the subchondral bone.

The aim of this thesis was to demonstrate migration mechanisms as part of the normal physiological remodeling process between the subchondral bone and overlying hyaline articular cartilage. It was based on the hypothesis that the cells in the calcified cartilage layer are not hypertrophic, but very much alive and capable of proliferating and/or migrating through the tissue to maintain the cartilage. We also believe, that progenitor cells are constantly supplied by the subchondral bone and migrate through the calcified cartilage zone and the tide mark upwards into the cartilage matrix, where they continue to migrate to the cartilage surface along the collagen fiber network as part of the normal physiologic remodeling process.

Showing the migration of cells within the subchondral bone and cartilage unit was difficult, not only due to the lack of known technologies in literature of this field. Technical limitations of finding the right way to fix a live sample under the microscope and then penetrate it from either the cartilage or the bone-side or both, over a long time-period in a time-lapse microscope, while keeping the tissue alive, were a real challenge.

2 Literature Survey

2.1 Animals

Compared to other domesticated large animals, sheep are quite accepted as research animals in society. They are easy to handle, behave very docile, are not aggressive and lower in cost than horses for example. It is easy to keep sheep in nearly perfect natural

conditions, which makes it more acceptable ethically and ethologically. They are flock animals and need to be kept with one or more companions. Sheep feel best outdoors with hardly any supervision. Because of the easy management of sheep, the costs for housing and pasture can be kept very low. There is a big variety in breed through having different use for sheep. Wool, milk and meat production cause a biological and/or genetic diversity[5].

In this case, sheep were also easy to access because they were used for many different other studies[6-10] at the Musculoskeletal Research Unit, Zurich.

The size of the sheep`s humeral head easily allowed me to collect a great amount of samples out of just one front limb, which reduced my need of animals and also compounds the benefit of large animals.

Although the general thickness of, for example, a horse's cartilage is almost equal to the general thickness of human cartilage, the horses` calcified layer is greater[11] compared to the ones of sheep. Because the focus is on the calcified layer in this study, it is of great importance to have an animal model similar to humans. Still it is more acceptable to society to use sheep as research animals, because they are "food animals" and humans have a lower emotional attachment to sheep, than to companion animals[12]. Also, there are no evolutionary reasons, why cartilage of sheep should heal differently to other species, like humans, in fact their morphology is very similar.

Rodents for sure, financially would be a better solution. Compared to all other animals their epiphyses retain open with continued enchondral ossification a life-long though. Besides that, the movement characteristics are very different from human beings, which changes their load pattern on the cartilage. Another disadvantage of rodents is, that the joint size obviously is way smaller than in large animals and the cartilage layer is very thin. Different from humans and sheep, cartilage heals intrinsic spontaneously in rodents.

Even though financial aspects and public acceptance of ethical aspects have to be considered, large animal models address a lot of the limitations, which are linked to rodent models. Large animals are required for translational research, which is supposed to be used in human clinical trials, and are compulsory for the regulatory approval of cartilage repair strategies. More important than the size of animals is the maturity of the cartilage itself according to the ICRS (International Cartilage Repair Society). Mature cartilage ensures that biochemical, biomechanical and cellular healing characteristics are appropriate for human clinical application.[13]

The sheep that were used for this study were all female and aged between 2-3 years. Immediately after arrival from the farm (Staffelegghof, 5024 Küttigen, Switzerland), the sheep were examined by a veterinarian and adjudged as non-pregnant and free from disease. All research animals were maintained in good health.

2.2 Articular Cartilage

Cartilage in synovial joints is so-called hyaline cartilage. It is the most common cartilage in the body. Not only in joints, but also rib cartilage, as well as nasal cartilage and the cartilage rings in the trachea and the bronchial tubes consist of hyaline cartilage. Its name comes from the bluish color it has in early age. Hyaline cartilage has two known ways of growth. It grows from the inside through matrix synthesis (interstitial growth) and, in case of non-articular cartilage, from the outside through the perichondrium (appositional growth). It is said that mature cartilage stops its appositional growth and only carries on, in case of an injury.

Hyaline cartilage in general is covered with the perichondrium, which has two layers. The top layer, called stratum fibrosum, which helps to distribute the shear forces, the stratum chondrogenicum follows, which helps to regenerate the cartilage with its mesenchymal cells. The perichondrium is supplied with blood vessels that provide the cartilage with nutrients through diffusion. In joints, the perichondrium is only left at the transition from periosteum to the cartilage region, but there is no perichondrium covering the hyaline cartilage on the articular surface. Here, the hyaline cartilage is not supplied with blood, but gets its nutrients through diffusion out of the synovial fluid[14].

2.2.1 Cells

Compared to other tissues in the body, the metabolic activity of cartilage is very low[15]. The cartilage varies in thickness, depending on the location, the species and the type of joint. In most cases, it is in humans between 1-5 mm thick, in sheep thickness is between 0.3 – 0.9mm (own measurements). The only cells found in articular cartilage so far, are called chondrocytes, which only make up 1% of the articular cartilage volume in human adults[16].

2.2.1.1 Chondrocytes

Chondrocytes are usually shaped round. Depending on their location (zone) they also appear ellipsoid or flattened[17]. Chondrocytes lie in so-called chondrones, which include not only the cell itself but also its surrounding environment (described in 2.2.3.2). The chondrones are situated along the collagen fibers. They are isolated from other cells, blood vessels and nerves. Being metabolically active cells, they produce the extracellular matrix, consisting of collagens, glycoproteins, hyaluronic acid and proteoglycans[17]. Still their metabolism varies according to their location in articular cartilage[18].

2.2.1.2 Cytoskeleton and cell migration

The cytoskeleton of cells is not only important for keeping the shape of the cell upright, but also plays an important role regarding load and interaction with its surrounding matrix. The main components of the 3D mesh in chondrocytes are f-actin, vimentin and tubulin[19].

F-actin is mainly found circular (Figure 2.1.a), like a ring around the cell, while vimentin is found between the nucleus and the cell membrane (Figure 2.1.e). Tubulin (Figure 2.1.i) is spread through the whole cytosol[20].

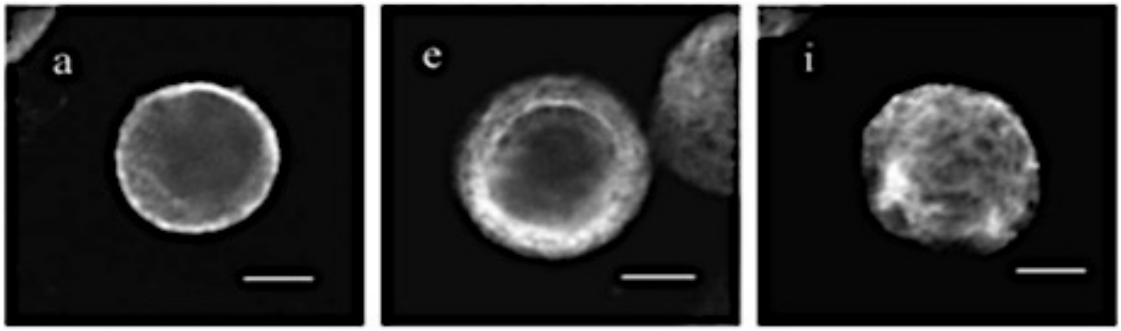

Figure 2.1. F-actin (a), vimentin (e) and tubulin (i) labeled with fluorescent (source: Trickey et al. [20]).

The actin skeleton changes actively as soon as a cell migrates. In general, cells, which are capable of migrating, follow four basic steps. At first the cell needs to polarize, in order to know where its front - which will move forward - and its rear is. The main role in polarization belongs to the actin filaments, which orientate themselves towards the leading margin and are mainly responsible for the movement of the cell.

In the back of the cell, myosin II causes retraction. Myosin II is depended on actin. It is still not known which exact mechanisms cause polarization in cells, but it is very clear that it can be caused by multiple ones.

The second thing that happens is protrusion. As the actin filaments, at the front of the cell, start forming bundles in order to form filopodia, or when they crosslink to form lamellipodia, they actually start pushing the cell forward. While forming the protrusion, the actin filaments up front are detached from the ones facing the rear part of the cell. As soon as it is formed, the protrusion needs to bind to the surrounding matrix. This third step, the adhesion, is caused by integrin, which connects the end of the actin fibers to the outside matrix. In order to move the whole cell forward, the back part of the cell needs to now retract. The last step of cell movement is based on contraction of myosin II and the detached actin filaments, which are also called "stress fibers". The rear part is released from the matrix and can now move forward while the protrusion stays in contact with the outside surrounding matrix. Now the cycle of cell migration can repeat[21].

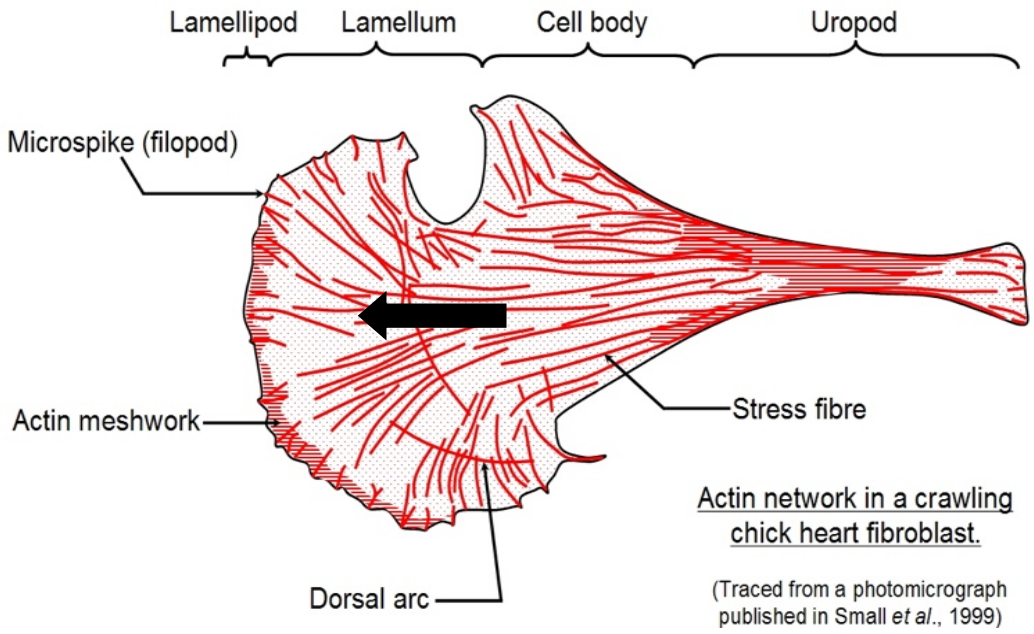

Figure 2.2. Arrangement of actin fibers forming the actin skeleton of a cell during protrusion. The arrow indicates the direction of movement (source: Small et al.22).

2.2.2 Tissue

Articular cartilage in synovial joints needs its special 4-layer structure (zones) in order to ensure its unique mechanical and metabolic behavior.

2.2.2.1 Zones

The hyaline cartilage has different zones (Figure 2.3) in which the cells and matrix components vary. Especially in the upper and the lower zones the amount of cytoplasmic cell organelles is increased (for example Golgi apparatus and endoplasmic reticulum)[23].

2.2.2.1.1 The superficial zone

The *superficial zone* (tangential) is the thinnest articular cartilage zone that makes out about 10% of the cartilage thickness[24]. It has a slim layer of ellipsoid-flattened chondrocytes that are organized parallel to the thin acellular layer, which covers them. The acellular layer is a sheet of fine fibrils with very little polysaccharides[15]. Through this layer, the cartilage is clearly separated from the immune system. The superficial zone has the highest water content[25] but a relatively low content of proteoglycan[26]. The collagen fibers in this layer have a diameter of about 35nm[24].

2.2.2.1.2 The transitional zone

The *transitional zone* follows. In this zone, the structure is completely different. The cells are shaped much rounder than in the superficial zone and are not as crowded. The zone has much more volume than the superficial zone. The cells have more organelles and the content of proteoglycan is increased in this zone[26] . Collagen fibers in this layer are thicker and have a diameter of about 60 nm[24].

2.2.2.1.3 The radial/deep zone

In the *radial zone* the chondrocytes are clearly arranged in columns. This zone has the least amount of cells. Compared to the other zones, the water content is the lowest and the amount of proteoglycans is highest[26]. The collagen fibers have the largest diameter with about 80 nm[24] and pass through into the *tidemark* that separates the non-calcified cartilage zones from the calcified layer[15].

2.2.2.1.4 The calcified cartilage zone

The *calcified cartilage zone* is the link between subchondral bone and cartilage. Depending on the author, the calcified layer is either part of the cartilage or the

subchondral bone plate[4]. The cells in this zone have less volume than the others and are often surrounded by calcified cartilage and packed in calcific caverns. These caverns, also called lacunae, contain no proteoglycans at all[26]. In humans, over the age of 60, the calcified layer decreases in thickness, while the number of tidemarks is increased[27]. Large collagen fibers cross the tidemark and reach into the calcified cartilage, while there are no collagen fibers described crossing the cement line, which separates the calcified zone from the subchondral bone plate[28,29]. Small blood vessels from the subchondral bone reach into the calcified layer through channels[4].

2.2.2.1.5 The tidemark

The *tidemark* is the separating line between radial zone and calcified cartilage. It is a narrow and wavy line and was first described as "tidemark" in 1953 by Fawns and Landells[30]. It is a very active metabolic area, in which chondrocytes and blood vessels are found occasionally. There are collagen fibers that do not only cross the tidemark and connect with collagen fibers in the calcified cartilage, but lie parallel to it and surround the whole tidemark area[31]. Also, the tidemark has an important biomechanical function. As a result of micro fracture for example, it merges into the uncalcified cartilage[4]. In cases of rheumatoid arthritis or osteoarthritis it appears, that the tidemark lines duplicate[32].

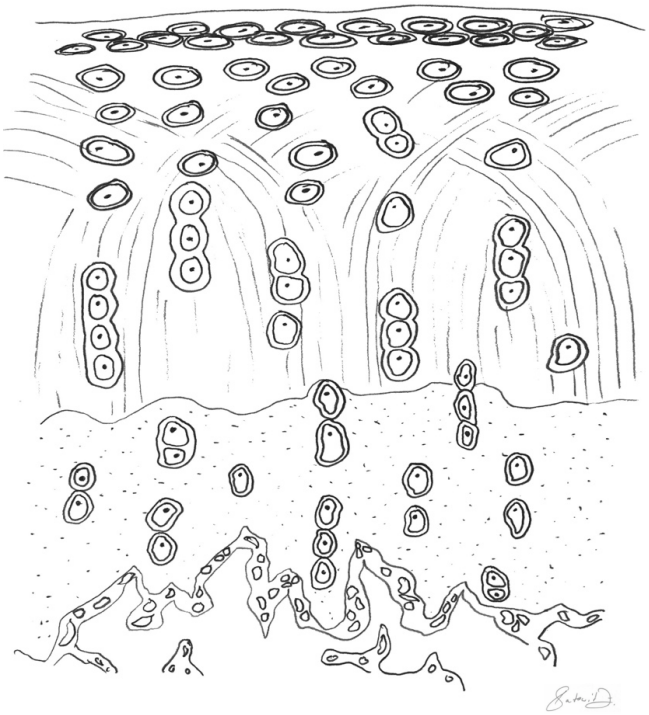

Figure 2.3. Zones of articular hyaline cartilage. (Illustration by Serah N. Saitowitz).

2.2.3 Matrix

Although there are cells in cartilage, the extracellular matrix is the main component[33]. The matrix mainly consists of water (about 75 %), proteoglycans and collagens. Collagen fibers and proteoglycans make up most of the dry mass[33]. Hyaline cartilage has 45 % less collagen fibers than fibro-and elastic cartilage. It is not supplied with blood vessels or nerves[15]. Chondrocytes often are found in isogenous groups, surrounded by proteoglycans (chondrones). In old age, hyaline cartilage seems to fossilize, because the thickness of the calcified layer increases.

2.2.3.1 Collagen

Collagen forms the framework for all the other matrix components[18]. The arrangements of the fibrils vary, depending on the zone they are in. In the superficial layer, the fibrils are orientated parallel to the joint surface, the content is higher[18] and the diameter of the fibrils is about 31 nm. In the middle/radial zone, collagen is arranged in arcades, which are called the "arcades of Benninghoff", and have a diameter of 40-100 nm. The fibrils of the deep zone have the largest diameter and hit the calcified layer vertically by crossing through the tidemark.

Articular cartilage has many different types of collagen. They can be divided in fibril-forming and non-fibril-forming collagens. With 90-95% occurrence[15], type II is definitely the most common collagen type in articular cartilage. It is produced by chondrocytes. Type IX and XI, as well as V and VI are known as the minor collagens, which contribute to the meshwork of type II collagen. Depending on the region around the chondrocyte, the collagen thickness and compositions vary.

2.2.3.2 Chondrones and their regions

Every chondrocyte lies in a chondrone[34], which is matrix and a capsule surrounding the cell. This matrix protects the chondrocyte hydrodynamically during physiological load[26]. There are single cell, double cell and multiple cell chondrones (linear cell rows). The articular pole of a chondrone faces the articular surface; the opposite side is the basal pole, facing the tidemark. In multiple cell chondrones, the basal poles merge. Chondrones have different regions, depending on the distance and zone location of the cell. The matrix components vary. There is the pericellular region directly surrounding the chondrocyte and acting as a protection for the cell or the cell groups[15,28,35]. Fine collagen fibers form a tight mesh around the cell. It preferably contains type VI collagen, which connects

directly with the cell surface[36,37]. It is exclusively found in the capsule of chondrones and is not a usual part of the territorial or interterritorial matrices[36]. Also, Aggrecan (= chondroitin/keratan sulfate-containing proteoglycan), link protein, cartilage matrix proteins and hyaluronate are found in this region[37].

The following region is called territorial matrix. It contains high concentrations of chondroitin sulfate rich proteoglycans. Collagen fibers, which are thicker than in the pericellular region, form bundles. The fibrils seem to connect with the pericellular matrix[38]. Adjacent to the territorial matrix one finds the interterritorial matrix, which contains an even greater diameter of collagen fibers and a higher amount of proteoglycans than the territorial matrix. This matrix zone has the largest distance to the cell and mainly contains collagen type II, IX and XI.

Single cell chondrones, the smallest ones, are mainly found in the middle layer of articular cartilage. Double cell chondrones are most often seen in middle and deep zone, they consist of two separate chondrocytes, which are associated with one and the same capsule. Also, multiple cell chondrones are found, which are basically three or more single cell chondrones linked to each other and are found in the deep layer. Type IV collagen surrounds all chondrones but is not as present between the adjacent chondrones[36].

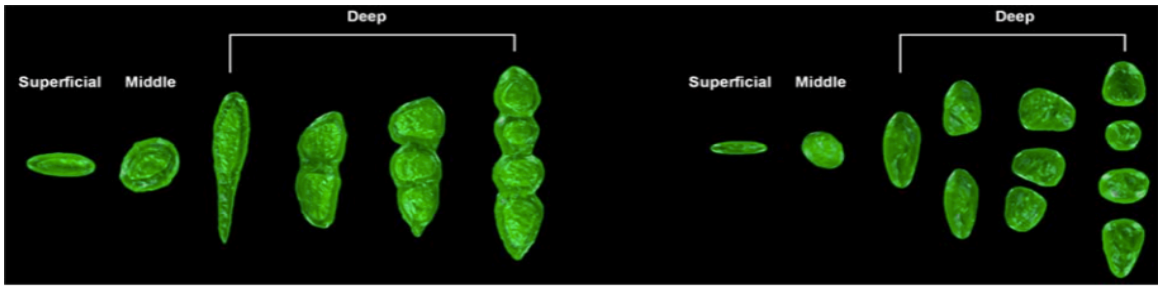

Figure 2.4. Different shapes of chondrones and chondrocytes in the different zones of articular cartilage (source: Youn et al. [39]).

2.3 Subchondral Bone

The articular cartilage is based on the subchondral bone with the calcified cartilage zone as a transitional zone. As already mentioned before, it depends on the author whether the calcified layer is part of the cartilage or part of the bone[28]. Basically, it has two different functions: *(i)* to spread all the pressure and shear forces caused through mechanical load equally on to the bone and *(ii)* to give contour and stability to the articular cartilage[18]. The subchondral bone consists of the subchondral bone plate and the below lying subchondral trabecular bone, which is subarticular cancellous bone. It is separated from the articular

cartilage through the calcified zone by the cement line. The articular cartilage in turn is separated from the bone marrow through both layers of the subchondral bone[4].

The top layer, directly in contact with the cartilage, is the subchondral bone plate. This layer borders the subchondral trabecular bone. The subchondral bone plate consists of cortical bone, in which the haversian system runs parallel to surface, not like in diaphyseal cortical bone, where it runs vertical to the joint surface[18]. In contrast to articular cartilage one finds a lot of blood vessels and nerves in the subchondral bone plate. The number of blood vessels and their modeling activity in the calcified zone is different depending on load and age[40]. Through small channels, in which the blood vessels run, the calcified cartilage can be reached directly[4]. Because these channels are not spread out equally, some parts of articular cartilage are dependent on diffusion of the synovial fluid as its only source of nutrition[4]. The number of channels varies from joint to joint[40]. The thickness of subchondral bone is different, also depending on joint localization but also species[4].

Collagen fibers from cartilage never cross into the subchondral bone, but abruptly stop at the cement line[29].

It is important to know, that mesenchymal stem cells are found in the subchondral bone. In case of full-thickness defects, where the subchondral bone is included in the injury, these cells can differentiate to chondrocytes, which finally are able to produce matrix and repair the lesion, although with lesser quality than the original hyaline cartilage[41].

2.4 Chondrocyte migration

It is known that chondrocytes are able to migrate in cell cultures within planar or three dimensional matrices[42]. What is not yet proven though, is that chondrocytes also migrate in an explant, which keeps its physiological structure, like in the body. Chondrocytes need to defeat the pressure and density of the matrix to be able to move. They might be able to do this with the help of their actin skeleton[42]. It was already shown by Lee and Loeser (1999) that chondrocytes are able to "grab" collagen fibers that are close by or even lie directly on the cells and change their shape in order to move forward[43]. Type II collagen fibers are often bent sharply, while type I collagen fibers are rather gently curved by chondrocytes within 48h after adding the fibers to the cells. The chondrocytes manage to "grab" the fibers actively and pull them close to the cell body. They seem to get in "contact" with the fibers with micro spikes or a cilium[44]. It was proven that the bending of collagen fibers was only possible with the presence of β1-Integrin[43]. Most of the

chondrocytes have a cilium which can change the cell metabolism by being bent. Integrins like α1, α2 and β1 are found all over the cilium[44].

2.4.1 Growth plate versus articular cartilage

In the metaphysis of long bones, during youth, you can find a hyaline cartilage plate, also called the epiphyseal plate, physis or growth plate. The growth plate, which consists of hyaline cartilage, is the region in which endochondral ossification takes place. There are different zones in the growth plate. The zone of reserve contains quiescent chondrocytes at the epiphyseal end. The most active chondrocytes are found in the zone of proliferation where they undergo constant mitosis accelerated by growth hormone. Further above in the zone of maturation, the chondrocytes become hypertrophic, and mitosis is stopped. Now the cartilage starts to calcify, which causes apoptosis of the cells. The calcified cartilage is replaced by osteoblasts and osteocytes in the zone of ossification. After puberty, the growth stagnates. An increase of estrogen causes the apoptosis of the chondrocytes and ends the bone growth. The growth plates are fully resorbed and replaced by bone[45]. In adolescents, all that remains is an epiphyseal line.

Because the growth plate consists of hyaline cartilage and has a calcified zone, similar to hyaline cartilage in joints, it is assumed that the cells behave the same way. This is the reason for the assumption that cells below the tidemark, in the calcified cartilage layer of articular cartilage behave like chondrocytes in the growth plate and are slowly progressing to "terminal differentiation", hypertrophy and death. Hypertrophic cells increase their size and change their shape. Additionally, the cells in the calcified cartilage produce collagen X and stage specific matrix[46]. Although the role of collagen X is not clear yet, it is known that it is produced during calcification of cartilage and chondrocyte hypertrophy[47] in the growth plate. The main difference between growth plate and articular cartilage is, that the cartilage becomes bone during endochondral ossification and calcifies. The growth plate undergoes continuous vascular invasion and endochondral ossification until skeletal maturity.

Separating the calcified from the non-calcified cartilage the tidemark is an undulating line, which is only found in hyaline cartilage. In adults or non-growing joints the tidemark is most prominent and can duplicate as a result of inflammation or increasing age. The tidemark is in joints from the beginning on, and can be found in the growth plate from time to time.

2.4.1.1 Difficulties

To copy the *in vivo* situation of chondrocytes in articular cartilage and in order to track the cells in their natural surroundings, osteochondral explants have to be not only harvested in a way that cartilage and subchondral bone do not separate, but also without damaging the cells.

Currently it is impossible to recreate an artificial osteochondral interface that is three-dimensional. The culture of cells in two-dimensional models is too simple and ignores many known parameters, which cells need for proliferation for example and for homeostasis of the tissue. Especially mechanical aspects but also the interaction between cells as well as between cells and matrix are not given in two-dimensional models. Three-dimensional models would be the solution. Until now there is no common way to create a 3D osteochondral model and still be able to visualize activity on a cellular level. It is difficult to recreate a tissue with different cell types in different zones, especially without causing that these cell types dedifferentiate. Besides that the matrix of the subchondral bone is completely different from the chondrogenic matrix[48].

Cartilage tissue is harvested and cartilage explants are maintained *in vitro* in order to keep the chondrocytes within their natural three-dimensional matrix, which we are presently unable to replicate. Harvesting a cartilage explant with adjacent subchondral bone is one step further in ensuring that the environment of the osteochondral interface is maintained as close to that found *in vivo* as possible.

To visualize live cells *in vivo* or in vitro within a tissue or an organ, as it is the case in osteochondral explants, a dye is needed, which is minimal invasive and does not affect the functionality of the cells. The use of viral vectors expressing GFP as a transgene is a good way to stain live cells with green fluorescence. The fluorescence proves the cells viability as they need to produce the transgene, which allows the tracking of cells containing the produced GFP protein. Despite the embedded proof of viability, viral vectors are very invasive, especially regarding the metabolic activity each cell goes through in order to constitutively express GFP. Other stains specific to the cell membrane or intracellular proteins such as actin may be less invasive. Their presence however does not inherently prove cell viability and an additional viability test must be performed.

To date, there is unfortunately no chondrocyte-specific stain available, which labels live cells and persists with cell proliferation. For future *in vivo* cell tracking studies, new solutions must be found to both target and reliably tag a cell within its native tissue

environment. Such a tracking molecule could then possibly be delivered intraarticularly to allow specific cell labeling.

Besides the issues regarding the tissue itself, tracking chondrocytes over a certain amount of time in 3D using Confocal Laser Scanning Microscope (CLSM) need a steady setup of the sample with no movement of the explant itself, in order to track single cells within the tissue. Without affecting the explant and causing irritation of the cells, it is very challenging to fix the osteochondral slice to the bottom of a well plate. CLSM allows the imaging of fluorescence-tagged cells in a 3D tissue, with notable tradeoffs in resolution. One is then able to live track a cell movement within a 3D tissue over hours or days using time-lapse imaging. While fluorescent signal bleaching may be a concern in some cases, the laser influence on cell and tissue function over a longer time period within a time-lapse however has not been reviewed yet.

2.5 Articular cartilage degeneration

2.5.1 The process and landmarks of articular cartilage degeneration

It is a fact that articular cartilage starts to degenerate after injury has occurred. The loss of cartilage structure and function causes the clinical syndrome of osteoarthritis[49]. In turn, osteoarthritis is defined as a degenerative disease of the joint, hypertrophic or degenerative arthritis, which consists of a loss of articular cartilage with an attempt of repair as well as remodeling and sclerosis of the underlying subchondral bone[50].

Osteoarthritis is of great importance as it is a prevalent musculoskeletal disease in the world and one of the most common reasons for causing disabilities[51]. The first and main clinical changes in a degenerating joint are loss of cartilage, remodeling of subchondral bone and formation of osteophytes. Microscopically fibrillation and fraying of the top two layers of cartilage is observed. These irregularities of the cartilage surface can become clefts and even fissures, which can reach down to the subchondral bone. In sclerosis the subchondral bone stiffens up, which may cause delamination of the cartilage zones. In severe cases the cartilage may get over compressed due to the load on the joint and finally complete denudation of the subchondral bone may be caused[52]. In that case, blood vessels can break through the tidemark and cause it to multiply or thicken. The cartilage itself decreases its thickness through enzymatic degradation[53], although the matrix initially swells due to increasing water content.

Further during cartilage degeneration, one can find multiple chondrones lying together in one large lacuna[54]. These groups of chondrones are defined as clusters. Clusters are typical indicators for osteoarthritis. They are primarily found at the edges of the clefts or fissures in order to shorten the pathway of diffusion. Cluster formation is a result of chondrocyte proliferation[54], in turn chondrocytes in clusters still have the potential to proliferate[55]. Depending on the type of defect, the repair mechanisms are different.

2.5.1.1 Chondral full-thickness defects

In chondral full-thickness defects (Figure 2.5), the cartilage is disrupted. Because the full-thickness of cartilage is damaged, the subchondral bone is exposed but still intact. Canals through which tiny blood vessels reach into the calcified cartilage can be exposed.
In most cases, no fibrin clot can fill the defect, which causes a lack of inflammation. Still matrix macromolecules are synthesized and the cells proliferate. However, the newly produced tissue is not capable of filling the defect fully[56].

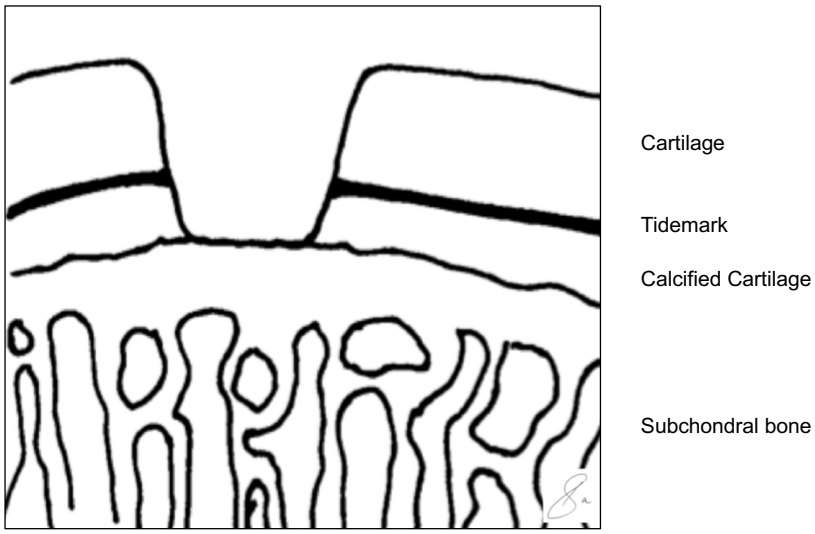

Figure 2.5. Chondral full-thickness defect (Illustration by Serah N. Saitowitz).

In case enough blood vessels from the calcified cartilage layer are exposed, the cleft can be filled with a fibrin clot tissue, which is produced by mesenchymal cells of the subchondral bone. In this case, the defect is replaced with either fibrocartilage or hyaline-like cartilage tissue.

2.5.1.2 Chondral partial-thickness defect

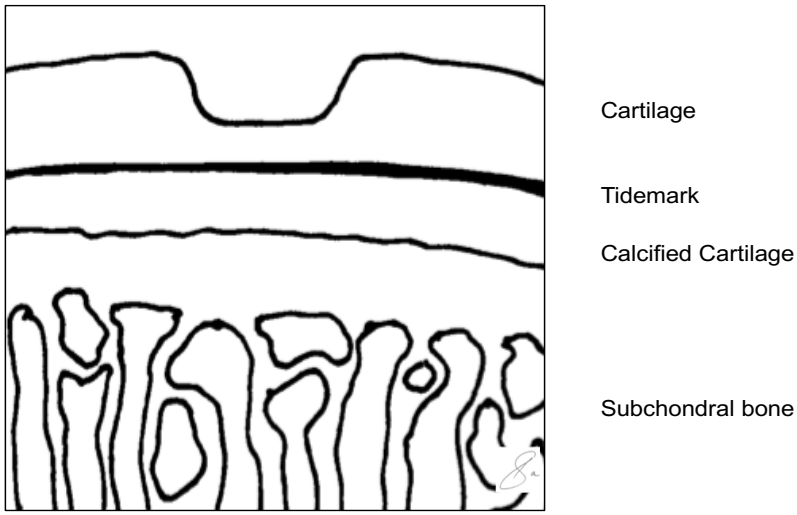

Figure 2.6. Chondral partial-thickness defect (Illustration by Serah N. Saitowitz).

Initially the subchondral bone as well as the cartilage below the tidemark is not affected through the injury (Figure 2.6). In this case the disruption of the surface is often not even visible. In this case, blood vessels from the subchondral bone cannot reach the defect. No typical way of healing can occur due to the fact that no fibrin etc. reaches the wound. In case the matrix basis is not destroyed and enough viable cells are available, cell proliferation as well as matrix synthesis takes place and healing may be possible depending on the size of the defect. If there is a lack of viable cells or the matrix basis structure is destroyed, the matrix will change its properties and no healing will take place[56].

2.5.1.3 Osteochondral defect

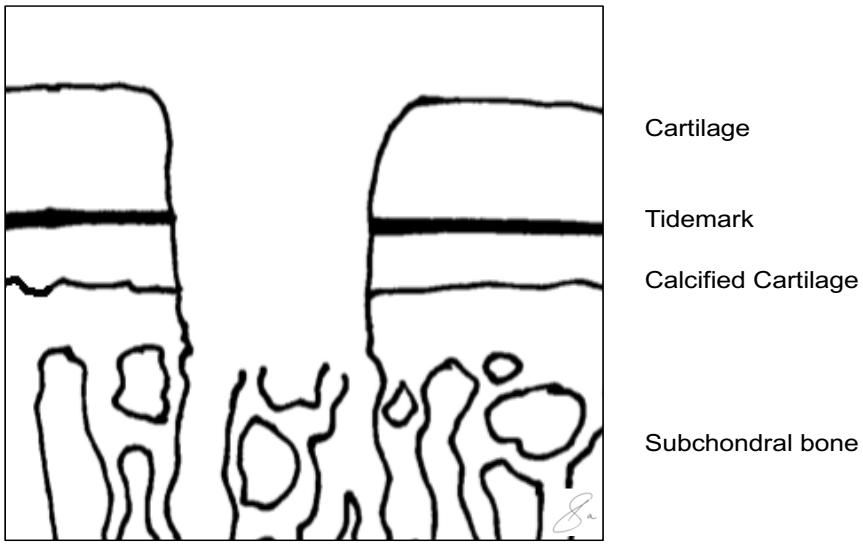

Figure 2.7. Osteochondral defect (Illustration by Serah N. Saitowitz).

Here the subchondral bone is part of the defect and the bone marrow cavity is exposed (Figure 2.7). In this case, blood vessels are also affected and blood as well as inflammatory factors can reach the defect. In this case the defect can be filled with a fibrin clot containing pluripotent undifferentiated MSCs, which then can differentiate into chondrocytes and osteoblasts through present growth factors[4,56]. Inflammation takes place, the new cells invade the region of defect and the healing pathway can proceed.
Very often though, lesions of this size do not heal, but tend to progress due to load and movement[56].

2.5.2 Failure of articular cartilage healing

The main two reasons for the failure of healing in articular cartilage are, that first of all, not every disruption of the tissue leads to denudation down to the subchondral bone and subsequent bleeding and thus to a fibrin clot following inflammation and production of new cells and tissue; second, the process of cartilage healing takes time and is, due to its very strained position in the body, not always able to heal in time, before the load or movement of the joint causes the defect to deteriorate and increase[56].

3 Material and methods

3.1 Study design

The methodology used in this thesis expanded on the work described in the thesis of Dr.med.vet. Sophie Schöberl[1]. The main aim was to demonstrate the migration of cells from subchondral bone into the articular cartilage.

3.1.1 Method establishment *in vitro*

The method was established using osteochondral explants, which were taken from the humeral head of the shoulder joint of sheep. These sheep were slaughtered for other, unrelated experiments, and the harvest of tissues for this thesis did not have an impact on the study design of the other experiments. Similarly, the treatments applied to the sheep, from which the samples were taken, did not impact the tissues harvested for the experiments described herein. The details of the other experiments are not described in this thesis for confidentiality reasons. Once the fresh osteochondral explants were harvested, they were prepared as 200-300μm thick slices that could be microscopically imaged in the CLSM. Various cell tagging methods were tested as well as special agarose filled wells, which were designed to culture the tissue explants and track the cells movement within using time-lapse imaging with the CLSM. Explants were also stimulated with pro-inflammatory substances to promote their migration and proliferation.

3.1.2 *In vivo* experiment

Once the method was established *in vitro*, an *in vivo* experiment was conducted in a sheep model. Briefly, a standardized metaphyseal defect in the proximal tibia was created in one stifle joint of 4 sheep, just 4mm below the cartilage surface. Two of the sheep received post-operative transdermal application (TDA) of an anti-inflammatory drug, while two did not receive any treatment after surgery. The osteochondral explants harvested from these four sheep after sacrifice were used to investigate cell migration through the calcified cartilage zone, and the impact of inflammation on osteochondral cell behavior.

3.2 Experimental animals

All samples for the *in vitro* establishment of the method were taken from healthy female sheep, after sacrifice. The animals did not show any obvious changes in cartilage or bone while harvesting the explants, therefore the tissue was considered healthy at the time of harvest. The animals were all between 12 and 36 months old (average of 24 months).
For the *in vivo* part of this study with the metaphyseal defect 4 healthy female sheep at the age of 24 months (born 03/2014) were operated and samples were taken from the cartilage layer above the created metaphyseal defect in the tibia. The tissue harvested in this case was expected to have undergone some level of degeneration, which may have been partially rescued by the anti-inflammatory treatment. This animal experiment, which required an *in vivo* component, was conducted according to the Swiss laws of animal protection and welfare (Tierschutzgesetz (TSchG) 455) and authorized by the cantonal ethical committee under the license no. ZH165/15.

3.3 *In vivo* animal experiment

3.3.1 Medication/Substances/Materials

- Attane®, isoflurane (Piramal Healthcare Limited, Tamil Nadu, India)
- Chlorhexidin, (Mölnlycke Health Care AG Brandstrasse 24, 8952 Schlieren, Switzerland)
- Diclo Hyal TDA®, (Arivine Pharma AG, 8008 Zürich, Switzerland)
- HibiScrub®, (Mölnlycke Health Care AG Brandstrasse 24, 8952 Schlieren, Switzerland)
- Ketonarkon 100®**,** ketamine, (Streuli Pharma AG, 8730 Uznach, Switzerland)
- Midazolam Sintetica®, midazolam, (Sintetica S.A., 6850 Mendrisio, Switzerland)
- Penicillin Natrium Streuli®, benzylpenicillinum, (Streuli Pharma AG, 8730 Uznach, Switzerland)
- Piezosurgery®, (Mectron s.p.a., medical technology, 16042 Carasco, Italy)
- Propofol 1% MCT Fresenius®, propofol, (Fresenius Kabi AG, 4436 Oberdorf, Switzerland)
- Rimadyl®, carprofen, (Zoetis Schweiz GmbH, 8052 Zurich, Switzerland)
- Temgesic®, buprenorphin, (Indivior Schweiz AG, 6340 Baar, Switzerland)

- Tetanus-Serum®, equine tetanus antitoxin, (MSD Animal Health GmbH, 6000 Lucerne, Switzerland)
- Vetagent®, gentamicin, (MSD Animal Health GmbH, 6000 Lucerne, Switzerland)
- Vitamin A® Augensalbe, retinol, (Bausch & Lomb Swiss AG, 6301 Zug, Switzerland)
- Xylazin Streuli®, xylazine hydrochloride, (Streuli Pharma AG, 8730 Uznach, Switzerland)

3.3.2 Pre- and Perioperative Treatment

After the animals arrived at the Musculoskeletal Research Unit (MSRU) in Zurich, they were examined and weighed by veterinarians. Blood samples were taken 2 days after arrival, to check the general condition of the sheep and to make sure the animals were in healthy for anesthesia purposes. The only parameter, which was slightly increased, was creatinine kinase (CK). However this is normal shortly after transportation.

	Control		Diclofenac	
Animal ID	54.01	54.04	54.03	54.06
Weight	54,8 kg	69,0 kg	56,9 kg	62,7 kg

Table 3.1. Bodyweight of sheep.

All animals were fasted for 24 hours before surgery. During this time, they only had access to water ad libitum. Before surgery, the animals were examined thoroughly by a veterinarian and then received premedication such as xylazine (xylazine hydrochloride 0.1mg/Kg BW) and buprenorphine (buprenorphine HCl 0.01 mg/Kg BW) intramuscularly. After 20-30 minutes, the skin in the region of the jugular vein was clipped and cleansed in a sterile manner. Then a catheter (14 G) was placed into the jugular vein and fixated with suture material. Further medication was given for pain control and antibiosis (carprofen 4 mg/Kg BW, gentamicin 4 mg/Kg BW, penicillin 30000 IE/Kg BW (= 0,06 mL/Kg BW) intravenously and tetanus serum (3000 IU/ Dose= 3 mL/animal) was given subcutaneously.

For induction of anesthesia, the animal was brought to the operation room. Here the animal received ketamine (3-5 mg/Kg BW), midazolam (0,1 mg/Kg BW) and propofol (0,4-0,6 mg/Kg BW or as needed) through the jugular catheter. After waiting a few minutes the animal was placed in sternal recumbency. An assistant stretched the neck and opened the mouth, so that the anesthesiologist could see the larynx with help of a

laryngoscope and spray it with Lidocaine. After about 90 seconds the tube was placed in the trachea and was cuffed and then tied to the jaw. The animal was placed on the surgery table and the tube connected to the anesthesia machine. The anesthesia was maintained with inhalation of 1-2 Vol% of isoflurane in oxygen and a constant-rate infusion with propofol was administered.

On the surgery table the sheep was placed in lateral recumbency. The upper hind limb was padded with a bandage just above the fetlock joint and then tied in flexion to the left table side in cranio-dorsal direction (Figure 3.1).

Figure 3.1. Positioning of sheep during the surgery (Illustration by Serah N. Saitowitz).

In this position, it was easy to approach the medial side of the hind limb stabilized firmly on the table on an inflatable mat. The limbs were clipped and cleansed in a sterile manner (chlorhexidine and HibiScrub, Mölnlycke Health Care AG, Switzerland).

3.3.3 Surgery procedure

An incision of about 8 cm was performed at the medial aspect of the tibia shaft extending from the middle of the stifle joint at the height of the patella down to the metaphysis of the proximal tibia. Bleeding was controlled with electro cautery. The soft tissue and fascia were incised. A wound retractor was used to expose the site of the planned defect. The space between the medial meniscus and the proximal rim of the tibia, as well as the lateral collateral ligament of the stifle joint were identified and marked with hypodermic needles (Figure 3.2). The needles were placed into the joint space carefully in order to not

harm the cartilage. The two needles (20 G x 1 1/2") were placed to determine the slope of the tibia plateau.

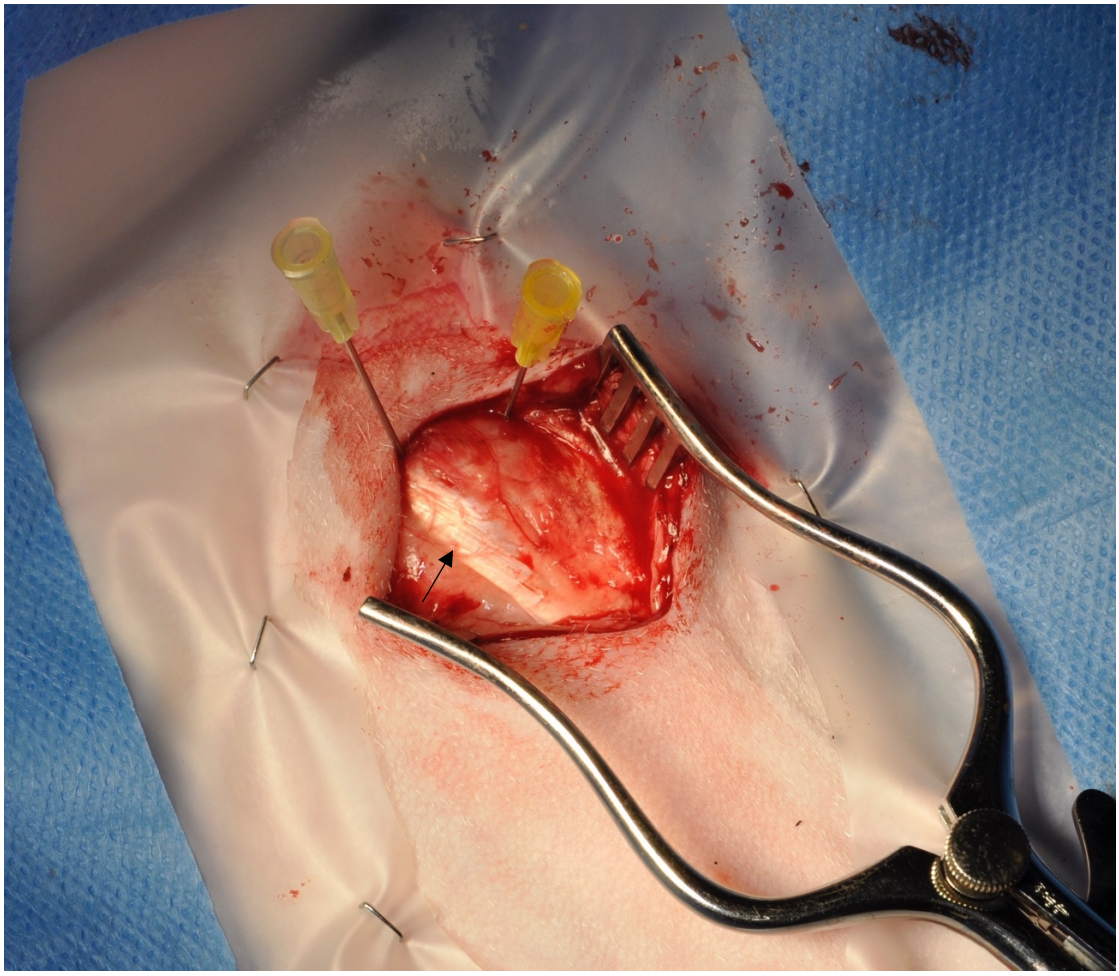

Figure 3.2. Surgery field with needles marking the rim of the tibia plateau. The arrow indicates the collateral ligament (CL).

The soft tissue was dissected down to the bone cranially to the collateral ligament. The periosteal elevator was used to cleanse the bone of all adhering tissue.

A prepared metal template of 1.0 cm height, and 1.5 cm width was adjusted to mark the planned defect region directly cranially of the collateral ligament and 4 mm below the proximal rim of the tibia (Figure 3.3). The distance from the rim of the proximal tibia was measured from the previously placed hypodermic needles, thus, placing the templates parallel to the slope of the tibia plateau. The outline of the defect was marked using electrocautery. Then the template was removed and the rectangular defect created parallel to the hypodermic needles using a piezoelectric surgery scalpel.

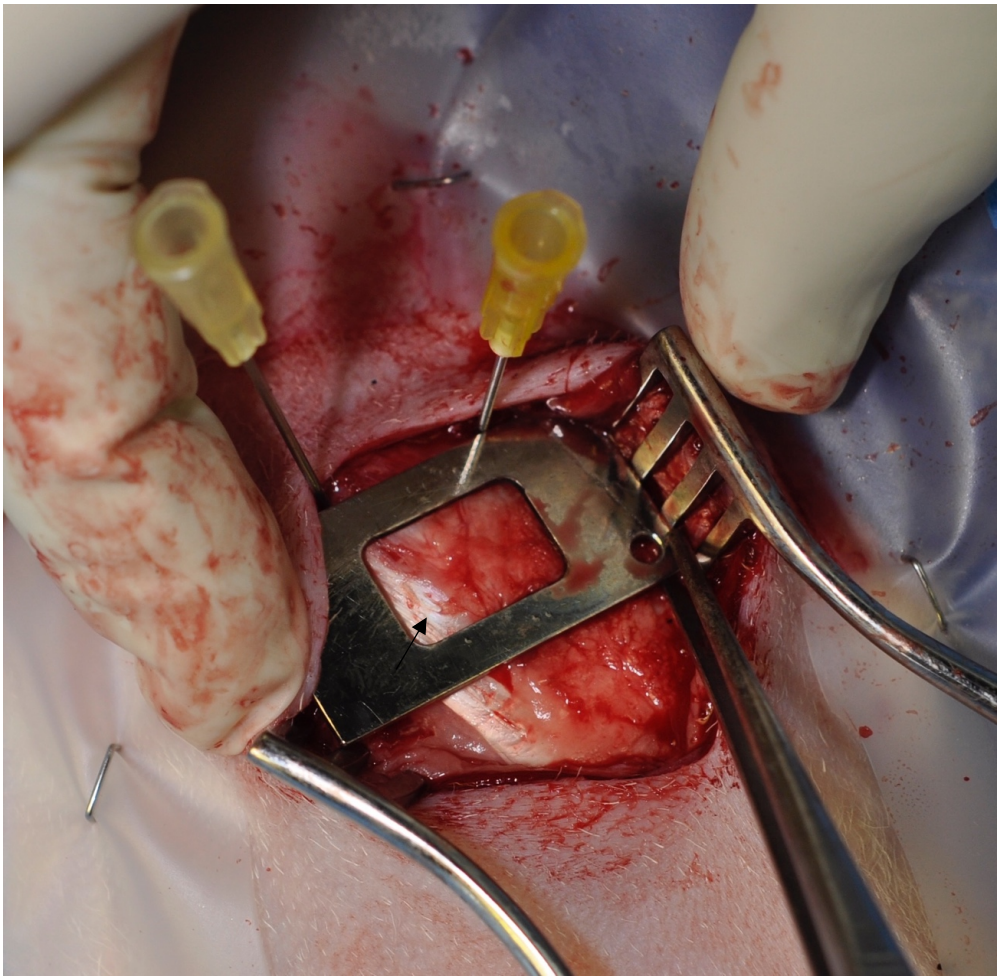

Figure 3.3. Placement of the template on the medial side of the tibia, in order to create the metaphyseal defect. The arrow indicates the CL.

Once the cortical slot was made, the bone block was carefully lifted. For this, a small osteotome was slid along the four walls of the cortex by carefully tapping on the tip of the osteotome with a hammer. Thereafter, the cancellous bone block was carefully removed and the desired depth of the defect was further deepened with the piezoelectric scalpel and curette (depth 1.8 cm). The depth of the defect was measured in all four corners with a depth gauge to assure adequate length.

The created tibia slot (Figure 3.4 (A)) was filled with the same bone that was taken out as a block (autograft) (Figure 3.4 (B)). Before filling it in, the extracted bone was crushed into small pieces with a rongeur. Then the wound was closed with degradable suture material (Vicryl, 2-0) and the skin with surgical staples.

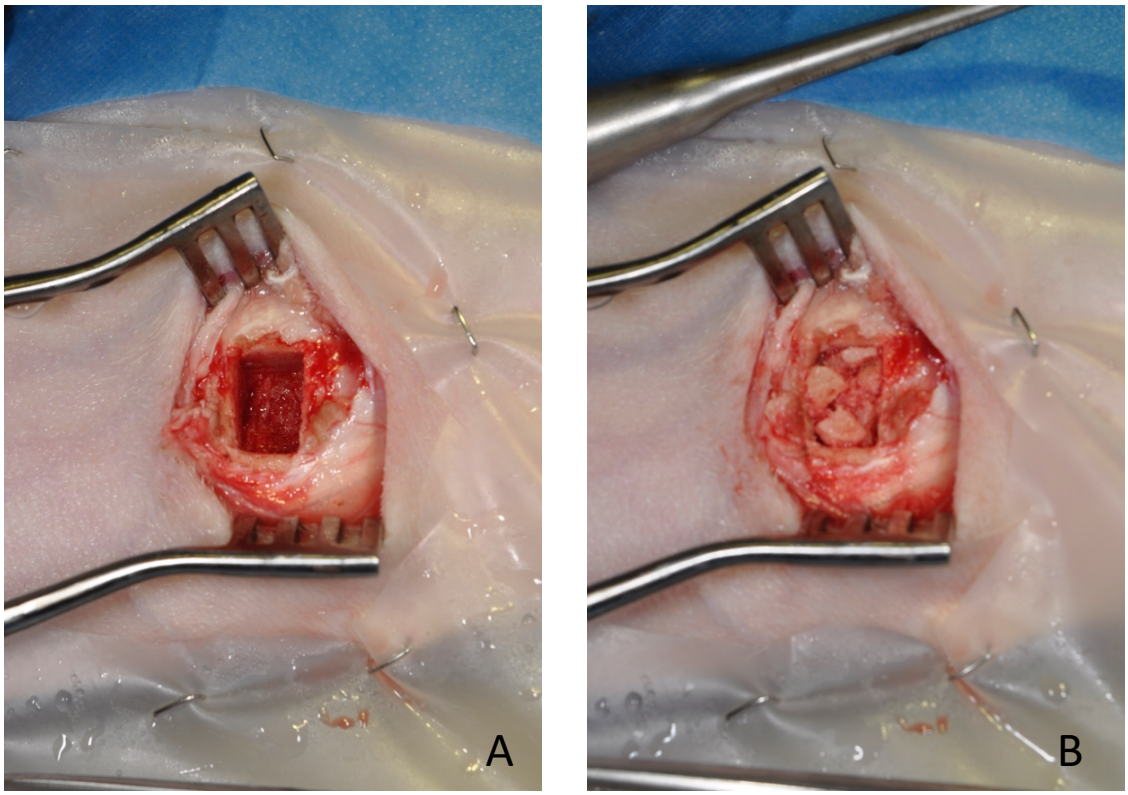

Figure 3.4. Metaphyseal defect in the tibia without (A) and with the created autograft (B).

3.3.4 Postsurgical treatment

After recovery, the animals were taken back to the stable, where they received food (hay twice per day) and water (ad libitum). No further stabilization of the limb was needed. According to our monitoring procedure, the sheep received analgesics (buprenorphine 0,01 mg/Kg BW) every four hours for a total of four times (including the one application before surgery) on the day of the surgery. Twelve hours after the first application of penicillin, the animals received a second dose intravenously (30000 IE/Kg BW). The operated animals were treated with penicillin, gentamicin and carprofen for a total of five days post-surgery including the day of surgery.

The sheep of the "Diclofenac Group" got 1 mL of Diclo Hyal TDA® transcutaneous immediately after surgery and then daily for 14 days. The TDA-system allows transcutaneous application of substances, which are bound to liposomes and oxygen as carrier materials. It is "blown" onto the area of the joint space with this special Meddrop device. The TDA system consists of an air compressor and a hand-held device for the application. The compressor extracts oxygen from the atmosphere and this high concentrated oxygen serves as a carrier substance for the anti-inflammatory Diclo Hyal TDA®. The oxygen stimulates and transports the carrier substance under pressure, while

also mixing with it. The system causes a so-called Venturi-effect (in response to a constricted flow area the fluid pressure decreases), so the micro emulsion is atomized. The drops, which hit the skin, are in the nanometer range dimension regulated by the needle at the end of the device. The substances are based on oil-in-water or water-in-oil microemulsion. The active ingredient is transformed into a watery phase, so it can bind with adjuvants and the surface tension of the drop is broken. Now the active substance can be dissolved without binding particles[57].

The sheep's limb was always clipped in the region of treatment and cleansed with ethanol before application. The substance was applied onto the skin in a 90° angle to the surface and a distance of about 1cm (Figure 3.5).

Veterinarians observed all sheep at least twice a day and their condition was noted in the impatient record of each animal.

Figure 3.5. Treatment of the metaphyseal defect with the TDA system.

	Diclofenac Group	Control Group
Life span	14 days	14 days
Treatment post-surgery	1mL Diclofenac daily	-
Amount of animals	2	2

Table 3.2. Groups for experimental animal model.

3.3.5 Sacrifice

Two weeks post-surgery, the animals were taken to the slaughterhouse of the Vetsuisse-Faculty in Zurich. They were brought into the slaughter room separately and stunned manually with a bolt. In order to stun a sheep, the bolt has to be placed in the middle of the head, behind the horn-basis of the animal and has to be aligned with the mouth. Immediately after the stunning (maximum stun to stick/kill interval is 60 seconds according to the Swiss law of animal protection VTSchS 455.110.2 attachment 2), the throat was cut and the sheep were hung at their hind limbs in order to bleed out as rapidly as possible. After bleeding, the limbs were detached of the carcass and were now ready for the sample harvest.

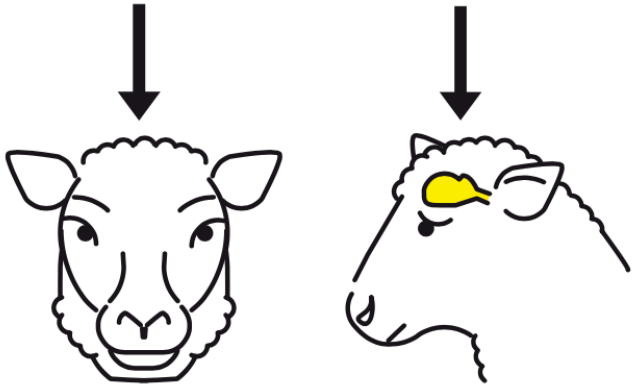

Figure 3.6. Position of the bolt for the stunning procedure of hornless sheep (source: Swiss animal protection law, VTSchS 455.110.2 attachment 2c).

3.4 Sample harvesting and processing

3.4.1 Sample extraction

Sample harvesting was performed under aseptic conditions. The skinned forelimb was separated from the corpus immediately after slaughtering, leaving the shoulder joint intact. The sample extraction itself took place in the veterinary anatomy institute of the Vetsuisse Faculty in Zurich, Switzerland.

For the *in vitro* establishment of the method, the samples were taken from healthy animals, sacrificed for other studies. The diaphysis of the humerus was wedged into a bench vice with the scapula facing up. The shoulder joint capsule was opened under sterile conditions and the head of the humerus was immediately irrigated constantly with sterile sodium chloride, so that the cartilage would not dry out during extraction. With the OATS® System (by Arthrex) and a hammer, explants (8mm diameter) were taken in a 90°

angle and immediately put into cold HBSS + 1% penicillin/streptomycin + 55mM sodium citrate in centrifuge tubes that were placed on ice.

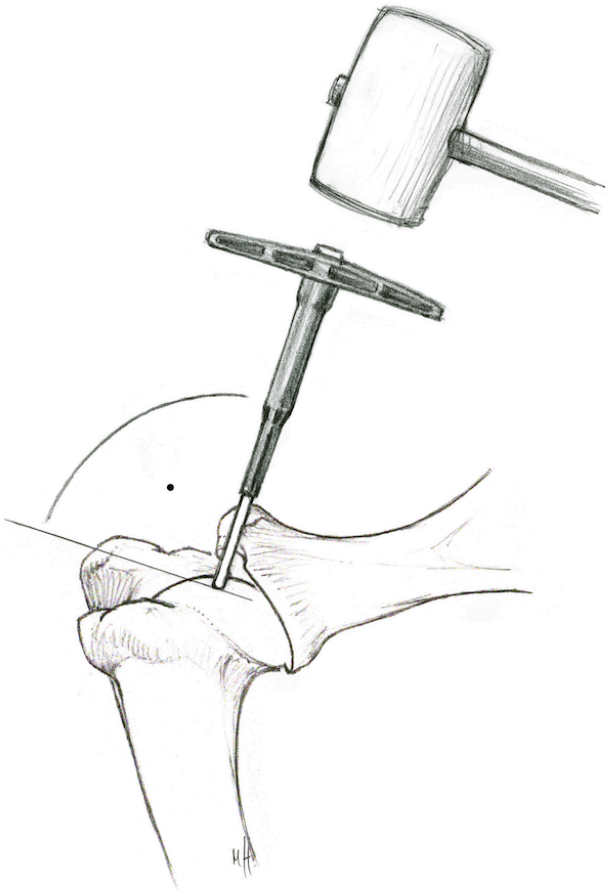

Figure 3.7. Illustration of sample harvesting with OATS from a shoulder joint (source: Schoeberl et al.[1]).

The exact same procedure was done with the operated sheep with the metaphyseal defects. The only difference here was that the explants were taken from the tibia plateau of the operated hind limb (Figure 3.8). The knee joint was approached under sterile conditions and the osteochondral plug taken from the tibia plateau in the region above the created defect. Explants were taken within the defect as well as some on the border of the defect.

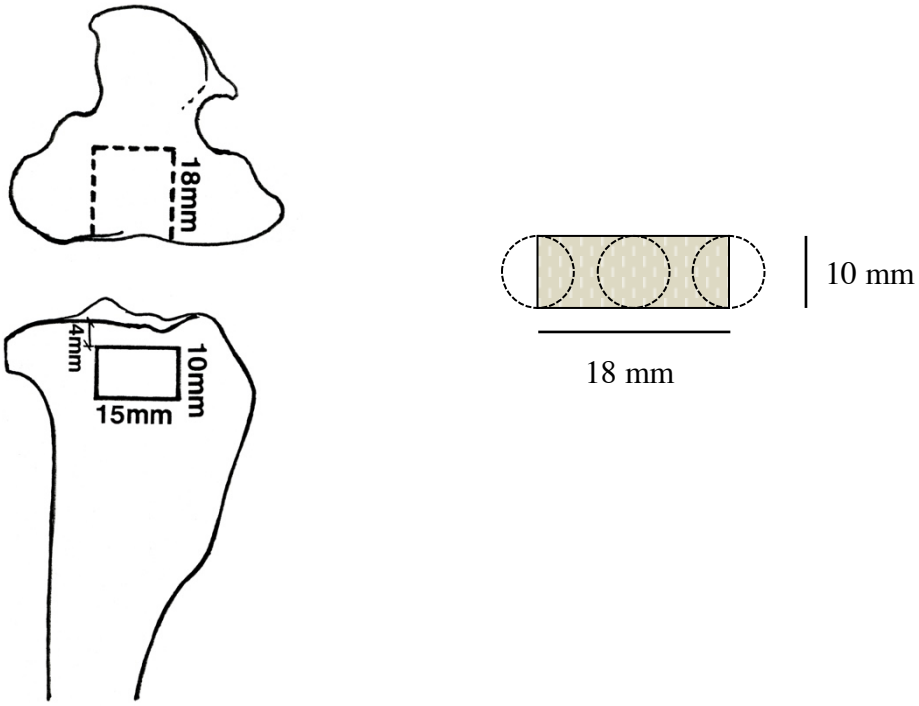

Figure 3.8. Illustration of metaphyseal defect region by M.Haab(left). Region of interest for harvesting plugs (right).

Due to the tibia slot, which was filled with autografts, it was difficult to take the osteochondral explants because the underlying bone would break away (Figure 3.9, Figure 3.10). Still it was possible to take the samples including the remaining subchondral bone.

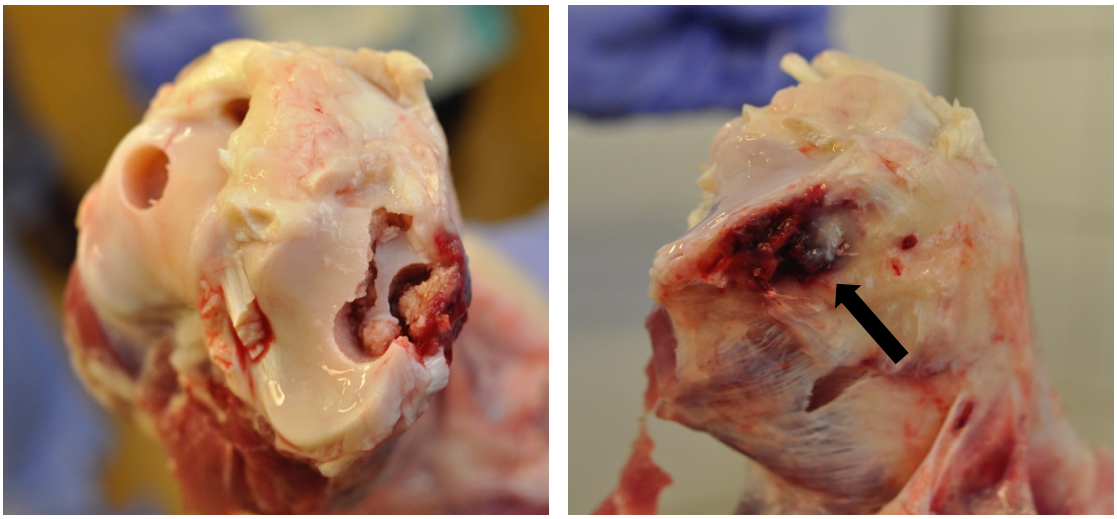

Figure 3.9. Tibia after harvest of osteochondral plugs (left image). Region of healed defect indicated by the arrow (right image).

Figure 3.10. Tibia plateau after harvesting plugs above the created metaphyseal defect.

3.4.2 Preparation

After harvesting the explants, they were washed in HBSS + 1% penicillin/streptomycin twice. Then the cancellous bone was taken off bit by bit with a hand rongeur until only the subchondral bone and the calcified cartilage zone were left (Figure 3.11). At the end, all plugs had a diameter of 8mm and were about 2 mm thick after removing the cancellous bone.

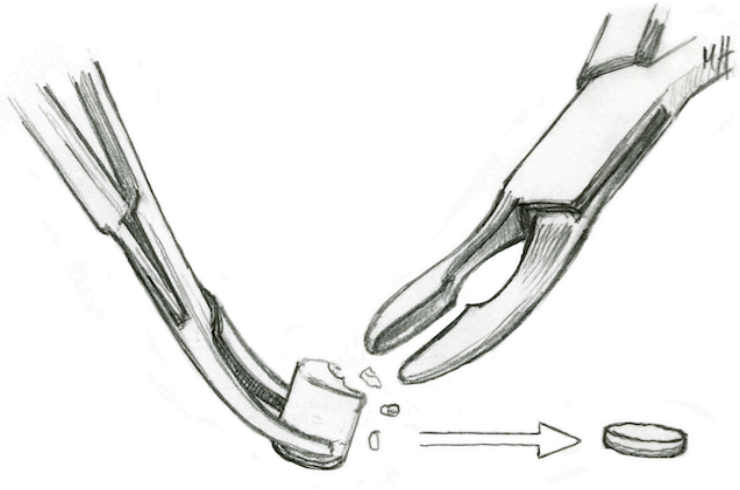

Figure 3.11. Breaking down the lugs with a hand rongeur (source: Schoeberl et al.[1]).

After washing the plugs again in HBSS + 1% penicillin/streptomycin and twice in pure sodium chloride they were put on a shaker for 30 min (250 rd/min) in HBSS+ 5% penicillin/streptomycin. They were then placed on the shaker again for 15 min in a tube with HBSS + 1% penicillin/streptomycin + 55mM sodium citrate. Thereafter, the plugs were cut into thin slices by hand with a sterile scalpel in a petri dish with PBS (Figure 3.12). The slices were about 2mm x 0,3mm x 1mm. The thickness of 300μm varied slightly, because they were cut by hand. Also, the width was not always the same because the plugs were round originally. After cutting the slices they were put back into complete cell culture medium (see below).

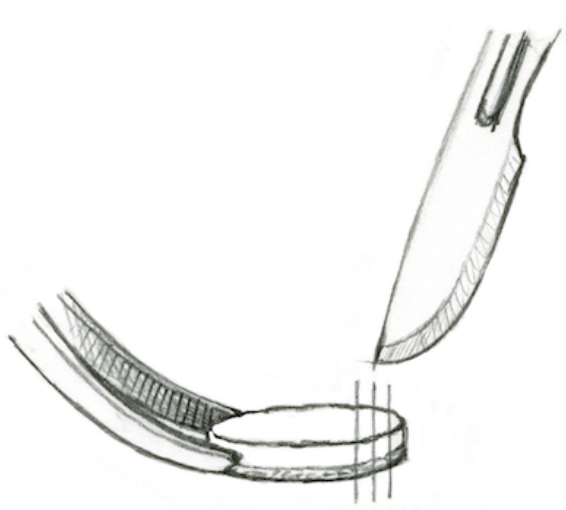

Figure 3.12 . Cutting slices of the harvested plugs (source: Schoeberl et al. [1]).

3.5 Explant Culture *In Vitro*

3.5.1 List of Materials

3.5.1.1 Chemicals and Reagents

- Amphotericin B (Catalogue no. A4888, Sigma-Aldrich Chemie GmbH, Buchs, Switzerland)
- Bovines Serum Albumin (Catalogue no. A2058, Sigma-Aldrich Chemie GmbH, Buchs, Switzerland)
- Dulbecco`s Modified Eagle Medium/F12 D8437 (Catalogue no. D8437, Sigma-Aldrich Chemie GmbH, Buchs, Switzerland)
- Ethanolum Ketonatum 70% (Catalogue no. 02-6000-08, Hänseler AG, Herisau, Switzerland)

- Fetal Bovine Serum (Catalogue no. 10437010, Life Technologies Europe B.V., Zug, Switzerland)
- Formalin 4% buffered (Catalogue no. 84-1951-05, Biosystems AG / J.T. Baker)
- Hank's Balanced Saline Solution (Catalogue no. 14175-053, Life Technologies Europe B.V., Zug, Switzerland)
- Lipopolysaccharides from *Escherichia coli* 0111:B4 (Catalogue no. L4391, γ-irradiated, BioXtra, suitable for cell culture) (Sigma-Aldrich Chemie GmbH, Buchs, Switzerland)
- Penicillin-streptomycin (Catalogue no. P4333, Sigma-Aldrich Chemie GmbH, Buchs, Switzerland)
- Phosphate buffered saline (Catalogue no. 10010015, Life Technologies Europe B.V., Zug, Switzerland)
- Sodium Chloride 0.9% (Catalogue no. AUST R 29745, Fresenius, Bad Homburg v.d.H., Germany)
- Sodium citrate tribasic dihydrate (Catalogue no. 71404-250G, Sigma-Aldrich Chemie GmbH, Buchs, Switzerland)
- (+)-Sodium L-Ascorbate (Catalogue no. 11140, Sigma-Aldrich Chemie GmbH, Buchs, Switzerland)

3.5.1.2 Instruments

- Benchtop pH-Meter (Mettler-Toledo Ltd., Beaumont Leys, Leicester, UK)
- Incubator Sanyo MCO-18AC (UV) (Sanyo Electric Co.; Ltd. Osaka, Japan)
- OATS®, Osteochondral Autograft/Allograft Transfer System (Arthrex, Naples, FL, USA)

3.5.1.3 Other Consumables

- Centrifuge Tubes 15mL (Catalogue no. 91017, TPP Techno Plastic Products AG, Trasadingen, Switzerland)
- Centrifuge Tubes 50mL (Catalogue no. 91054, TPP Techno Plastic Products AG, Trasadingen, Switzerland)
- Eppendorf Safe-Lock Tubes, 1.5 mL (Catalogue no. 0030120086, Eppendorf, Vaudaux-Eppendorf, Switzerland)
- IBIDI μ-Dishes, 35mm (Catalogue no. 80136-IBI, Vitaris AG, Baar, Switzerland)

- Serological pipettes (2; 10; 25; 50ml), (Catalogue no. 2mL, 86.1252.025, 10mL 86.1254.001, 25mL 86.1685.020, 50mL 86.1689.001 Sarstedt, Nümbrecht, Germany)
- Syringe Filter, 0.22μm, (Catalogue no. 99722, TPP Techno Plastic Products AG, Trasadingen, Switzerland)
- Tissue Culture Test Plates (6, 24, 96) (Catalogue no. 6-wells 92006, 24-wells 92024, 96-wells 92096, TPP Techno Plastic Products AG, Trasadingen, Switzerland)
- Vacuum Filtration "rapid"-Filtermax (Catalogue no. 99500, TPP Techno Plastic Products AG, Trasadingen, Switzerland)

3.5.2 Explant Culture in Growth Media

Osteochondral explants were taken from the humeral head of sheep or the tibia plateau with the Osteochondral Autograft Transfer System (OATS® by Arthrex) immediately after approaching the joint. These explants, or plugs, were placed into growth media, composed of Dulbecco`s Modified Eagle Medium/Nutrient Mixture F-12 (DMEM/F-12 by GIBCO®) with fetal bovine serum (FBS by GIBCO®), penicillin and streptomycin, amphotericin B and vitamin C (shown in Table 3.3). The explants were kept in a humidified atmosphere at 37°C with 5% CO_2 and the media was changed 2 to 3 times per week. The same culture procedure was used for osteochondral plugs and osteochondral slices made from plugs.

Ingredients for explant growth media	Amount in %
DMEM/F12	89
FBS	10
Penicillin/streptomycin, 100x Stock: (100 U/ml penicillin, 10µg/ml streptomycin)	1
Vitamin C, 1000x Stock (25µg/ml)	0.1
Amphotericin b, 1000x Stock (5µg/ml)	0.1

Table 3.3. Explant culture media ingredients.

3.5.3 Stimulation of cells with LPS

In this set of experiments, no treatment of the cartilage or tissue was performed *in vivo*. Only healthy explants were taken and all treatments and stimulations were done *in vitro*. Plugs were harvested from the healthy humeral head of the shoulder joint, after the sacrifice of these sheep for an unrelated study. The plugs were then cultured in growth media, then placed in agarose and stimulated with LPS before imaging, as shown in Figure 3.13.

Gram-negative bacteria, like Escherichia coli, are surrounded by a kind of casing, which gives the bacteria its shape. On the outer side of this, which is pointed to the bacteria's environment, the casing is covered with proteins[58]. Of these proteins, Lipopolysaccharide (LPS) covers almost three quarters of an E.coli bacteria. Bacterial mutants, which are unable to form LPS cannot survive[59]. Toxicity of gram-negative infections and inflammatory processes are mostly influenced and caused by LPS. Relating to other research, LPS does increase proliferation[60,61]. In order to give the cells a "kick-start" or to create a similar inflammatory situation as in osteoarthritis, LPS was added to the cell culture medium for certain time periods before imaging. 1 mg LPS from *Escherichia coli* 0111:B4 (γ-irradiated, BioXtra, suitable for cell culture) (Sigma-Aldrich Chemie GmbH, Buchs, Switzerland) was dissolved in 1 mL HBSS. In order to find the right dosage to cause stimulation but no damage to the cartilage and bone cells of the explant we tested LPS at a concentration of 1µg/mL and 2 µg/mL in growth media or growth media alone (control). For the dosage test, the explants were kept in contact with the LPS-containing media for 24h, 48h or 72h.

The LPS-stimulation *in vitro* experiment was set up according to the basic scheme below (Figure 3.13). Briefly, explants were kept in growth media for a short (2-4 days), mid (10-13 days) or long (18-21 days) period (Figure 3.14). Afterwards, LPS was added to the growth media for a total of 4 or 7 days. During the last 3 days of culture, samples were imaged using time-lapse microscopy, as described below in chapter 3.7.

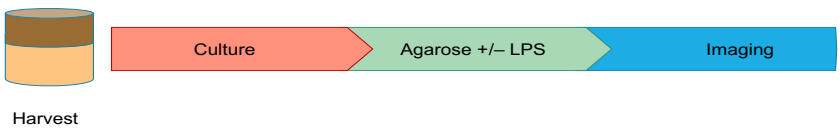

Figure 3.13. Overall setup of LPS stimulation experiments.

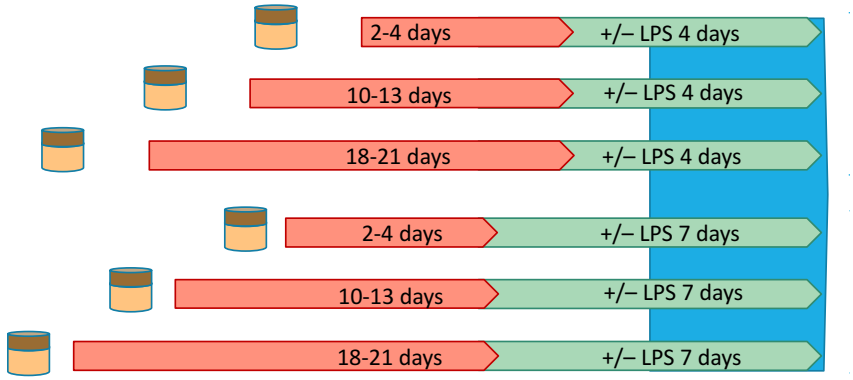

Figure 3.14. Detailed setup of LPS stimulation experiments, including culture times in growth media as well as stimulation times in LPS and imaging time frames.

Days in culture after harvesting	Short term: LPS total 4 days (added 1 day before imaging)	Midterm: LPS total 7 days (added 4 days before imaging)	Short term: No LPS	Midterm: No LPS
2-4 days	Group 3	Group 4	Group A	Group D
10-13 days	Group 5	Group 1	Group B	Group E
18-21 days	Group 2	Group 6	Group C	Group F

Table 3.4. Table summarizing the experimental groups for LPS-stimulation experiments.

3.6 Visualization of cells

In order to image cells in the CLSM, a few different methods were established.

The goal was to visualize cells with stains that would not influence the viability of cells in the osteochondral plugs. Staining multiplying and non-multiplying cells (which are in the resting phase G0, for example) was as important as keeping the signal for weeks.

3.6.1 List of Materials

3.6.1.1 Chemicals and Reagents

- Adeno Associated Virus-Typ2 NEO (Virology Institute, Francesca Franzoso, University Vetsuisse Zürich, Switzerland)
- CellTracker™ Blue CMAC Dye (Catalogue no. C2110, Life Technologies Europe B.V., Zug, Switzerland)
- CellTracker™ Green CMFDA Dye (Catalogue no. C2925, Life Technologies Europe B.V., Zug, Switzerland)

- Lentivirus Vector FUGW (Virology Institute Bruna Pareira/Anita Meyer, University Vetsuisse Zürich, Switzerland)
- Live/Dead Cell Viability Assay (Catalogue no. L3224, Life Technologies Europe B.V., Zug, Switzerland)
- Methanol (Catalogue no. BDH1135-1LP, VWR International GmbH, Dietikon, Switzerland)
- Phosphate buffered saline (Catalogue no. 10010015, Life Technologies Europe B.V., Zug, Switzerland)

3.6.1.2 Instruments

- Incubator Sanyo MCO-18AC (UV) (Sanyo Electric Co.; Ltd. Osaka, Japan)

3.6.1.3 Other Consumables

- Eppendorf Safe-Lock Tubes, 1.5 mL (Catalogue no. 0030120086, Eppendorf, Vaudaux-Eppendorf, Switzerland)
- IBIDI μ-Dishes, 35mm (Catalogue no. 80136-IBI, Vitaris AG, Baar, Switzerland)
- Serological pipettes (2; 10; 25; 50ml), (Catalogue no. 2mL, 86.1252.025, 10mL 86.1254.001, 25mL 86.1685.020, 50mL 86.1689.001 Sarstedt, Nümbrecht, Germany)

3.6.2 Cell labeling with viral vectors

Viruses have been used as therapeutics for more than 200 years, starting off with the aim to produce vaccines in order to prevent the smallpox disease. Besides the great interest in using viruses for vaccines, they are also often involved in gene therapy processes[62]. Part from this, viral vectors can also be used for visualization of cells.

3.6.2.1 GFP-AAV-vector

Adeno-associated viruses (AAV) were first discovered in 1960. They belong to the family of the parvoviridae and are replication-deficient. The genus is the so-called dependovirus, because they are *dependent* on a helper-virus or cellular stress to replicate and express genes. If no helper-virus is around, AAV can still infect a cell, but it will cause a latent infection, which can be activated by stress or super infection.

An AAV has an icosahedral shape. Its single-stranded DNA has approximately 4.7 kb. The genome contains two clusters of genes rep and cap which are flanked by so-called ITRs (inverted terminal repeats; Figure 3.15). Rep encodes for proteins, which are needed for replication, and cap encodes for proteins, which make up the capsid. The basis to produce an AAV vector is, that rep and cap can be deleted from the genome. The missing genes can be replaced by transgenes with control elements regarding the transcriptional process. When the AAV infects human cells, its genome remains episomal in the cell nucleus or is integrated into the host cell genome, preferentially at the so-called AAVS1 locus on chromosome 19. For this site-specific integration, the rep-proteins (replication) are required. The rtAAVGFP- Neo vector, which was used in this case, is totally apathogenic, as the rep part is removed from the vector, so it is non-integrating. The vector rAAVGFP Neo, has a small non-enveloped virus capsid with a diameter of 20-25nm[63].

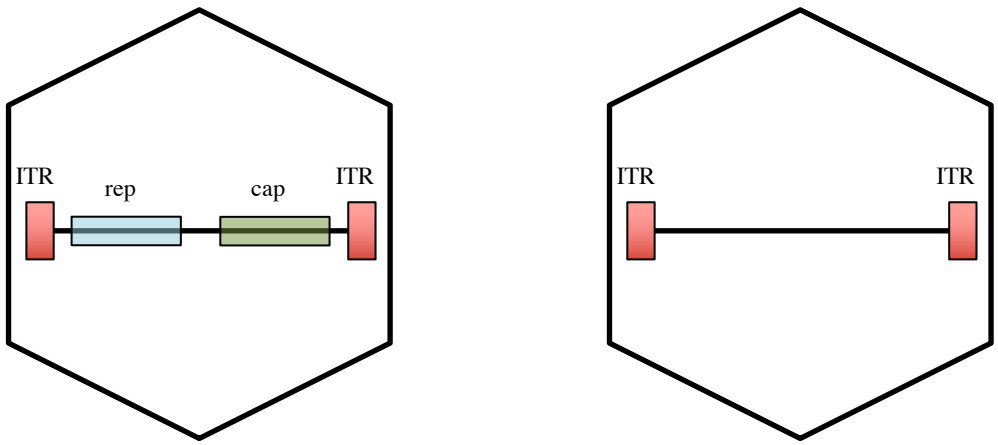

Figure 3.15. rAAVGFP-Neo genome.

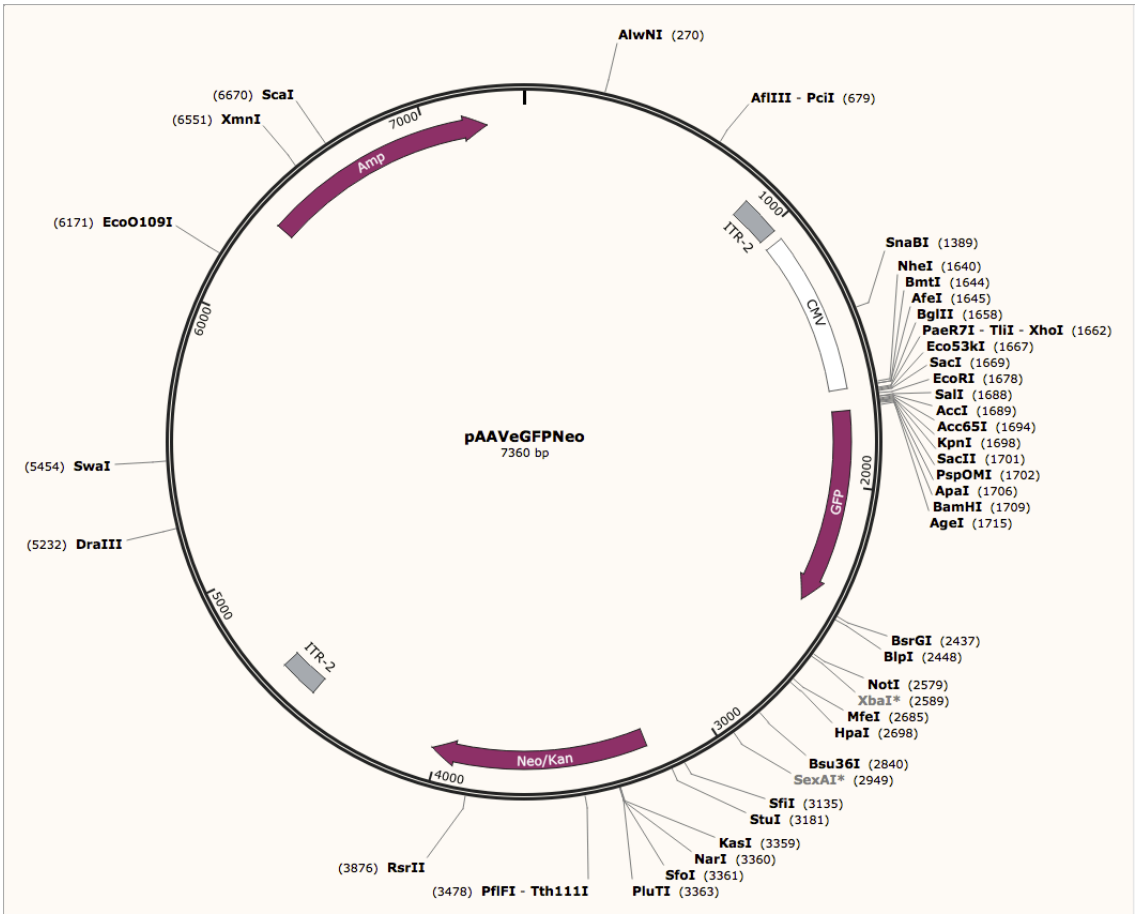

Figure 3.16. AAV-viral vector rAAVGFP-Neo (source: Dr.med.vet. Francesca Franzoso, dipl. ECVP, Virology institute Vetsuisse Faculty Zurich, Winterthurerstrasse 266a, 8057 Zurich, Switzerland).

3.6.2.2 Infection with AAV-Vector

The sliced explant samples in 100μL media (DMEM/F12) were placed into a 96-cell culture well plate. 20 μL of virus suspension were added to each sample. After infection with viral vectors the samples were incubated at 4 °C for 30 minutes in a fridge and then at 37°C, 5% CO_2 in a humidified standard cell culture incubator for 23 hours (MOI 5000). 24 hours post infection the samples were transferred into a six-well plate with each 6ml of complete media (90% DMEM/F12, 10% FBS, 1% penicillin/streptomycin (10.000 U/mL penicillin and 10mg/mL streptomycin), 0.1% amphotericin B (concentration 5 μg/mL) and ascorbic acid (concentration 25μg/mL)) per 6 slices.

To prove that the infection was successful, the cells were observed in the CLSM on the second, third and fifth day after transduction.

3.6.2.3 GFP-Lentivirus vector

Lentiviruses are a generic group belonging to the family of the retroviridae. Their name comes from the Latin word *lentus*, which means slow and was used because the period between infection and outbreak of the disease can take time. Lentiviruses are present in ungulates, such as horses, cattle, sheep and goats, as well as in felids and primates[64]. Unlike the other retroviridae, lentiviruses can regulate their genes by themselves. However, they do not have a "correction system", therefore mutations occur quite often. The probably most well-known lentivirus is HIV (Human Immunodeficiency Virus), which causes AIDS (Acquired Immunodeficiency Syndrome). In veterinary medicine the lentivirus is known for causing equine infectious anemia in equidae (EIA), as well as Maedi-Visna in small ruminants and feline immunodeficiency virus (FIV), which causes a similar syndrome in cats as AIDS in humans.

They are enveloped, + RNA viruses, with a length of 7-12 kb[65], which remain in their host during its lifetime. The virion has a diameter of 80-100 nm[66].

The three genes on the main segments are gag, pol and env, which code for proteins important for integration, replication and encapsulation of the virus[66]. There are further six genes, which also code proteins needed for replication, binding, infection and release (rev, tat, nef, vpr, vpu, Vif). Compared to conventional retroviral vectors based on Gammaretroviruses, the lentiviruses have the capability to infect non-dividing cells by overcoming the nuclear membrane[67].

The only safety concern is, that there is a possibility of activation of cellular oncogenes of the provirus into the host genome[68]. In order to prohibit these negative aspects, a self-inactivating expression vector (SIN) was used. This means, that a certain region (U3) was deleted to prevent the transcriptional activation of proto-oncogens[67].

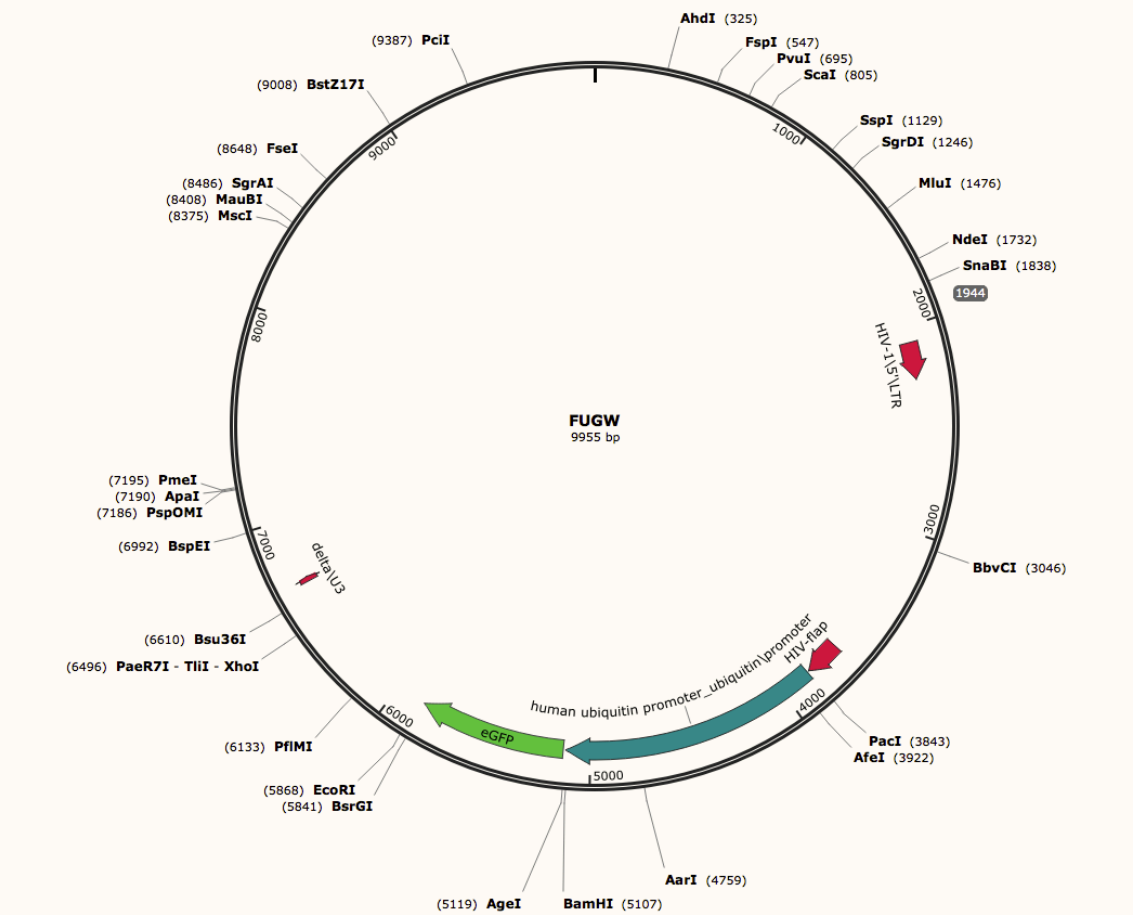

Figure 3.17. Lentiviral vector FUGW (source: Bruna de Andrade Pereira, PhD, Virology institute, Winterthurerstrasse 266a, 8057 Zürich, Switzerland).

3.6.2.4 Infection with lentiviral vector

In this study, we used the self-inactivating lentiviral vector FUGW (Flap-Ubiquitin-promotor-GFP and WRE-Vector) in order to express GFP in the cells within our osteochondral tissues.

After preparing the osteochondral explant slices they were placed in a 96 well plate with 100μL of non-supplemented DMEM/F12. 40μL virus suspension was added per well.

The virus titer was 1.6 x 10^7 gcp (genome-containing-particles) in 40μL. The samples were incubated for three hours at 37°C with 5% CO_2 in a humidified standard cell culture incubator. Afterwards, the fluid was aspirated and the wells were filled with 200μL DMEM/F12 containing 10% penicillin/streptomycin (10.000 U/mL penicillin and 10mg/mL streptomycin). The osteochondral slices were maintained in culture with a media change every second day. On the first, third and fifth day after the transduction, the cells were observed under the CLSM.

3.6.3 Cell labelling without viral vectors

3.6.3.1 Membrane staining with 5-chloromethylfluorescein diacetate (CMFDA)

Due to the uneasy handling of viral vectors, we decided to try out a membrane stain, which stains faster and lasts longer. For this stain, osteochondral plugs were harvested and cut into 300 μm slices by hand the same way as before.

After taking the slices out of the complete media, they were washed in PBS on a shaker twice for each 5 min. Then they were put into a 24-well-plate (2 slices per well) with 500μl DMEM/F12 media and 10μM of staining stock solution (= 1mg CMFDA in 215.1 μl DMSO) was added.

The covered well plate was wrapped in aluminum foil and incubated at 37°C, 5% CO_2 for 1,5 hours. Then the slices were taken out, washed in PBS twice for 5 minutes each, placed into complete media 90% DMEM/F12, 10% FBS, 1% penicillin/streptomycin (10.000 U/mL penicillin and 10mg/mL streptomycin), 0.1% amphotericin B (concentration 5 μg/mL) and ascorbic acid (concentration 25μg/mL). Slices were then imaged for 72 hours with the CLSM.

The stain was bright and it was not clear if it only stained the membrane or the whole cell. Due to the 3D sample of 300 μm, staining may be overlapping in the layers and was difficult to distinguish in the CLSM.

The stain lasted for a minimum of 14 days in culture.

3.6.3.2 Membrane staining with CellTracker Blue 7-amino-4-chloromethylcoumarin (CMAC) Dye 2

The idea behind using a blue stain was that one could lay a Live/Dead stain (green/red) over it. Like this we would have been able to prove if the blue stained cells were alive or not. With the CellTracker green CMFDA it was not possible to prove the viability of cells because one could not differentiate between the CMFDA green and the green of the live stain.

In order to create a stock solution 5mg of CMAC dye was diluted in 2,385mL DMSO. 10μM of this stock solution was then added to 500μL DMEM/F12 into a 24 well plate. Before this, the samples were washed twice in PBS for each 5 minutes on a shaker. The samples floating in staining media were wrapped up in aluminum foil to protect them from light and then incubated for 1,5h at 37 °C and 5% CO_2.

After 1.5h the samples were imaged in complete media (90% DMEM/F12, 10% FBS, 1% penicillin/streptomycin (10.000 U/mL penicillin and 10mg/mL streptomycin, 0.1% amphotericin B (concentration 5 μg/mL) and ascorbic acid (concentration 25μg/mL)).
The samples were kept alive for up to four weeks; in this time period the stain was stable.

3.6.3.3 Live Cytoskeleton staining with SiR Actin

When cells proliferate or migrate the actin skeleton changes its structure. With this stain, it was possible to make these changes visible, as it is based on the natural product jasplakinolide, which binds F-actin.
In order to create a stock solution with the concentration of 1 mM, the 50nMol of SiR Actin stain were diluted in 50μL DMSO. For time-lapse experiments a constant concentration of 100 nM was needed during the whole experiment. To reach this concentration 0.1 μL of stock solution need to be added per mL of complete culture media (90% DMEM/F12 (catalogue no. D8437, Sigma-Aldrich), 10% FBS (catalogue no. 10270106, Gibco), 1% penicillin/streptomycin (10.000 U/mL penicillin and 10mg/mL streptomycin; Sigma-Aldrich P4333), 0.1% amphotericin B (concentration 5 μg/mL, catalogue no. A4888, Sigma-Aldrich) and ascorbic acid (concentration 25μg/mL)).

3.6.4 Cell viability staining

Ingredients for Live/Dead staining	Amount in %
DMEM/F12	89
FBS	10
Penicillin/streptomycin, 100x stock: (100 U/ml penicillin, 10µg/ml streptomycin)	1
Amphotericin b, 1000x stock (5µg/ml) Only used on day 0-day 7	0.1
Calcein AM, 4mM in DMSO	0.1
Ethidium-homodimer-1, 2mM in DMSO	0.1

Table 3.5. Live/Dead stain working solution.

In order to determine cell viability within the explants, the LIVE/DEAD® Cell Viability Assay Kit (Calcein AM 40μL, 4mM in DMSO, Ethidium homodimer-1, 200μL, 2mM in DMSO) was used. The living cells are stained green, the dead ones red.
At first the staining media was prepared. For 300μL in total, 270μL DMEM/F12, 30μL FBS, 3 μL amphotericin B are mixed. 0.1% calcein AM and ethidium homodimer-1 were added in the end. The tube needed to be covered in aluminum foil immediately to protect the staining media from light. Then the samples were put in a 48-well-plate and 300μl of

staining media was added per well and sample. The samples were then incubated at 37°C, 5% CO_2 for 2 hours and kept in the dark as much as possible.
After two hours, the samples were taken out of the staining media and put into wells with PBS. The well plate needed to stay covered with aluminum foil to protect the samples from light, until they were imaged. When using the CLSM, the samples had to be placed in a suitable glass-bottom-dish to image them.

Lentiviral vector	CMFDA	SiR Actin	AAV vector
- GFP Transgene - Retrovirus - Requires BSL 2	- Green - Membrane stain	- Red - Stains live actin fibers	- GFP transgene - Parvovirus - Replication deficient

Table 3.6. Cell Labels summary of Characteristics.

3.7 Time-Lapse with Confocal Laser Scanning Microscopy

3.7.1 List of Materials

3.7.1.1 Chemicals and Reagents

- Agarose-gel, low temperature gelling (Catalogue no. A9045, Sigma-Aldrich Chemie GmbH, Buchs, Switzerland)
- Phosphate buffered saline (Catalogue no. 10010015, Life Technologies Europe B.V., Zug, Switzerland)

3.7.1.2 Instruments

- Confocal laser scanning microscope SP5 UV-VIS (Leica, Solms, Germany)

3.7.1.3 Other Consumables

- Glass-Bottom-Well plates (Catalogue no. P06-1.5H-N, Cellvis/BL Baustoff & Labor, 2201 Gerasdorf near Vienna)
- Serlim Wellinserts (Designed by Salim E. Darwiche, PhD, and Serah N. Saitowitz and built by Reto Maier, Physics Institute, UZH Zurich, Switzerland)
- Serological pipettes (2; 10; 25; 50ml), (Catalogue no. 2mL, 86.1252.025, 10mL 86.1254.001, 25mL 86.1685.020, 50mL 86.1689.001 Sarstedt, Nümbrecht, Germany)
- 16G x 1” Needles (Catalogue no. 4710016025, Henke-Sass, Tuttlingen, Germany)

3.7.2 Mounting of live explants in agarose

In order to take a time-lapse recording with the CLSM, and to track single cells in a sample, the osteochondral slice needed to stay in one place, so it does not move and influence the results of tracking. Developing half-moon shaped stainless steel well insert pieces made it possible to not only divide the well into two but also fix the sample to the plate with agarose.

Additionally, the agarose makes it more difficult for the cells to migrate out of the tissue and a separate stimulation from either cartilage or bone side can be reached.

After adding the low-gelling temperature agarose powder to sterile PBS in a beaker glass, it was carefully heated in a microwave under supervision, so it would not boil.

4% Agarose gel (1g Agarose was diluted in 25mL PBS)

Table 3.7. Agarose gel solution.

The 4% low-gelling temperature agarose (mixed with PBS) was cooled down to 37°C under the hood while constantly monitoring the temperature with a digital thermometer. Then it was filled into the wells containing the sample and the stainless-steel pieces with a sterile syringe and a 16 Gauge needle. After about 3 minutes the fluid agarose gelled. Then the stainless-steel pieces were removed and media could be filled into the well.

Figure 3.18. Serlim Wellinserts.

3.7.2.1 Agarose Test 1

The first Agarose well, was basically just a simple wall created through two Serlim Wellinserts the size of half the well. Here we used 12 well plates. Through using special low temperature gelling Agarose, covering harmed none of the cells[69]. We used 3% and 4% Agarose with PBS and filled it into the well right after the Serlim Wellinserts were placed in the plate with a syringe and a 16 G needle with a flow rate of 128 mL/min. The slice was covered at first in order to prevent the slice from floating up and letting Agarose get in between the glass bottom and the slice.

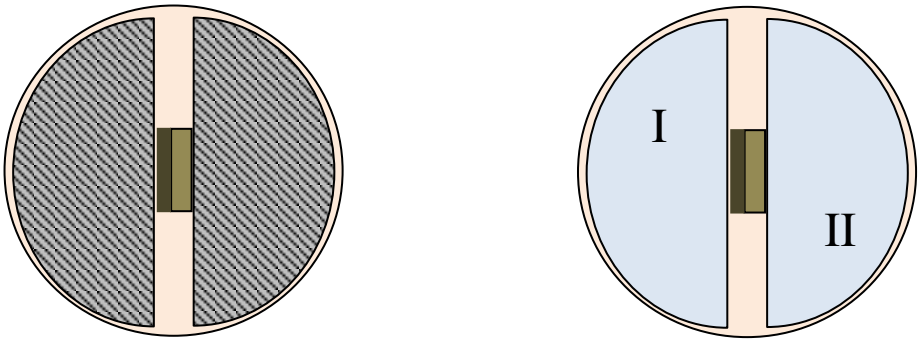

Figure 3.19: Well with two large Serlim Wellinserts, spaces filled with agarose, which then create two separated wells (I & II).

3.7.2.2 Agarose Test 2

Here the Serlim Wellinserts were shifted and put in a six well plate. We used 4% Agarose to strengthen the stability not only through increasing the amount of agarose but also the thickness of the wall.

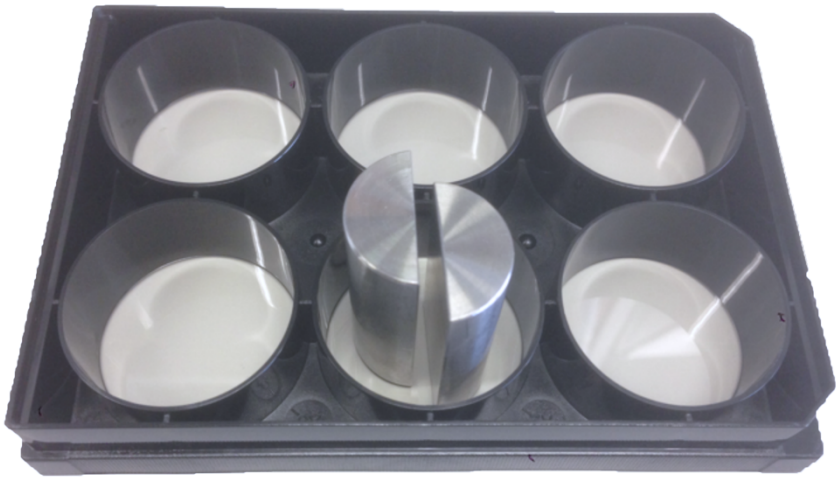

Figure 3.20. Glass bottom six well plate with Serlim Wellinserts.

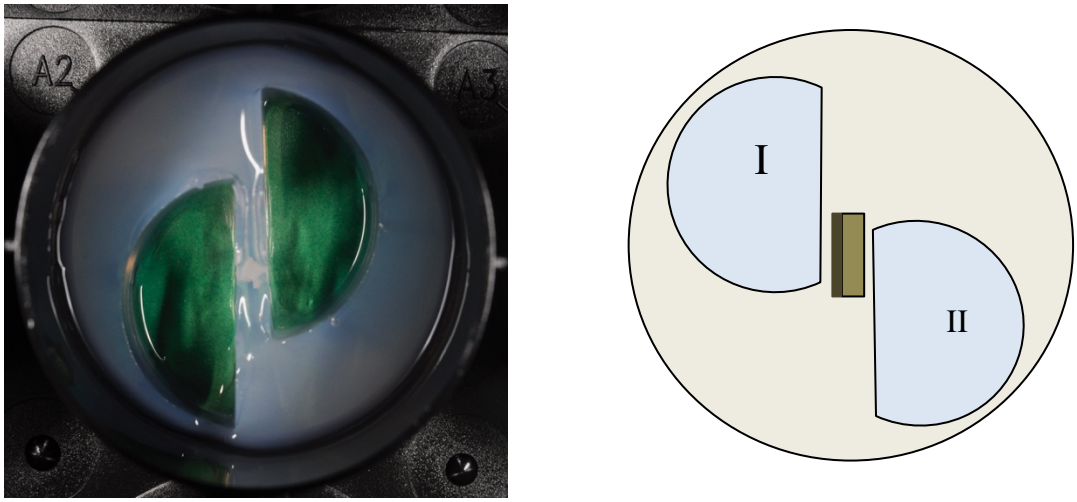

Figure 3.21. Agarose well with two separate chambers (I & II).

3.7.2.3 Agarose Test 3

To prevent the agarose from floating up in media and rotating within the well, we embedded additional stainless steel cylinders with a diameter of 2 mm and a length of 12 mm. We chose to embed 4 cylinders per well.

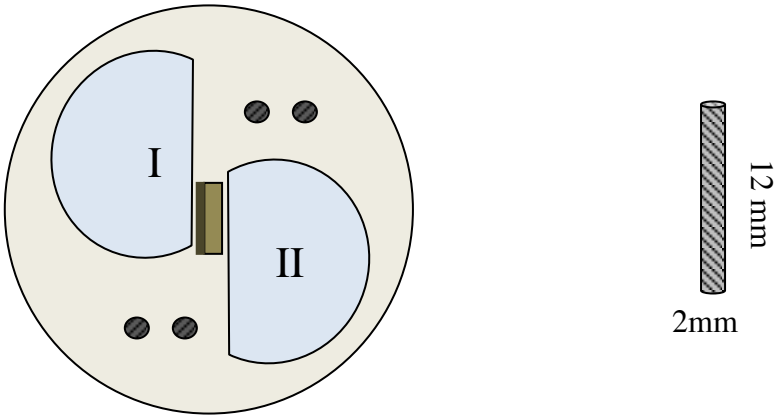

Figure 3.22. Agarose well with inserted cylinders to weigh down the gelled agarose.

3.7.3 Confocal Laser Scanning Microscope

Using a Confocal Laser Scanning Microscope (CLSM) made it possible to image the samples over a longer time-period. This microscope has a built-in incubator, which made it possible to keep the perfect temperature, humidity and CO_2-concentration constant while the samples were under the microscope. Only because of this it was possible to do the time-lapse recording. To produce optical sections through a three-dimensional sample, the CLSM is perfect[70]. The confocal laser-scanning microscope (CLSM SP5 UV-Vis) which was used, is located at the Zentrum für Mikroskopie und Bildgebung (ZMB), Irchel Campus UZH. The lasers can handle the depth of each slice much better than any other available microscope at the UZH.

Besides that, it is inverted and makes it possible to image the samples, which are placed on the bottom of the well plate, without having to go through all the layers of agarose. Like this there is nothing in between the laser and the sample, besides the glass bottom of the well plate. In order to reconstruct the three-dimensional sample and also to track possible cell movement through different layers, the z-stack imaging was very useful.

3.7.4 Time-lapse setup

To track the cells within a sample, the cells are stained and placed in the Agarose wells described in chapter 3.6.1.2. The six-well plate can be placed in the microscope with help

of a multi-well plate-insert. It is then covered with a special lid, which is connected to the CO_2. The temperature is set at 37°C and the CO_2 at 5%, so the cells can be imaged under the same conditions as within an incubator at the laboratory. Because there is no water basin in the microscope, a petri dish with a diameter of 200 mm was placed in the „incubator" and filled with distilled H_2O, to keep the humidity conditions upright. The distilled H_2O had to be refilled every day.

Depending on the stain that was used for the cells, the lasers are set (Table 3.8).

The bright field channel was also always used, so that the background tissue with the different cartilage layers was visible, to have better orientation while tracking the single cells.

Stain	Laser	Setting of Laser
Actin-stain	HyD4	633 nm at ca. 4%
CMFDA-stain	HyD2	488 nm at ca. 4%
Live stain	HyD2	488 nm at ca. 4%
Dead stain	HyD4	561 nm at ca. 8%

Table 3.8. Laser settings according to stain.

Before the time-lapse was started, multiple positions were set for each well. For each position, z-stacks were chosen and saved. Then the duration of the time-lapse, as well as the time interval was set. The total duration of a time lapse was set for 72 hours, with a time interval of 1 hour. The samples were all imaged with a dry objective that has a magnification of 10x. The resolution was set at 12 bit.

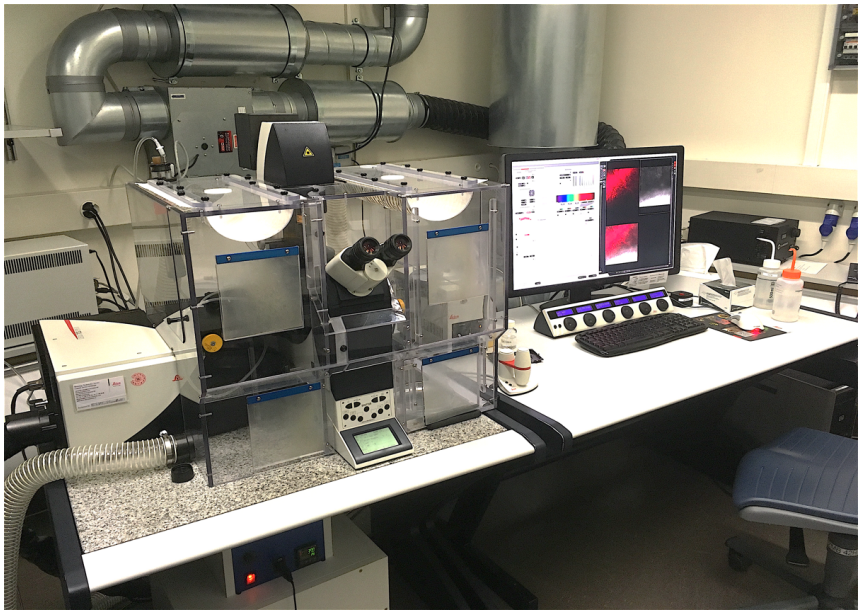

Figure 3.23. Confocal Laser Scanning Microscope SP5 at the ZMB, University of Zurich, Switzerland.

4 Results

4.1 *In Vitro* Explant Culture

4.1.1 Explant harvest and culture

The explant harvest and culture procedures were successful. Although the harvest procedure was done *ex vivo*, no microbiological contamination was observed. The washing procedure with antibiotics in PBS was therefore successful in preventing contamination throughout the *in vitro* experiments (manipulation, culture, time-lapse).
The method of harvesting plugs and producing thin osteochondral slices, although done manually, was consistently successful throughout the experiments across multiple harvests. This method, first established by Dr. med. vet. Sophie Schöberl[1], was successfully transferred and adapted to the experiments described in this thesis. This showed that the methodology was repeatable and successful also with different operators. The cells within the explants were viable after osteochondral sample harvest and throughout the culture period (up to 8 weeks). This was also the case when slices were produced from individual plugs, which showed that the designed growth media was compatible with osteochondral explant culture maintenance with media changes 2-3 times weekly. The culture conditions were appropriate for both osteochondral plugs and slices.

4.1.2 Sample mounting in Agarose wells

In order to image the cells within the explants over 72 hours it was most important to keep the sample immobilized and to prevent the flotation of the slices in its media during imaging. As described in methods, first, the osteochondral slice (200-300 μm) was fixed with a simple agarose wall, which went diagonally once across the well (35 mm in diameter). We were able to create this with the help of large Serlim Wellinserts. However, after removing the Serlim Wellinserts, the remaining slim agarose wall collapsed easily or floated and then tipped over when adding media. A thicker, 4% agarose (instead of 3%) was used to create more stability. This was not enough though because the wall would still wobble sideways, despite the thicker agarose. By using smaller inserts, and placing them in such a way to shorten the wall between both agarose wells, the stability was increased and the osteochondral slice would be placed within the wall (Figure 3.21). To keep the whole agarose structure from rotating within the 35mm well, stainless steel cylinders were embedded in the agarose to weigh down the agarose structure

(Figure 3.22). But these cylinders where not heavy enough and would easily escape the agarose after some days. Using sandpaper, the slick walls of each well plate could easily be roughened. This increased the friction between the agarose structure and the 35mm plastic well walls, thereby avoiding agarose rotation, even when the agarose was swollen with media, which usually would make it more slippery.

Because the heated agarose cooled down very quickly, keeping it at the perfect temperature while making the agarose wells was challenging. The agarose was poured into the well at 34-39°C, to avoid causing harm to the explants or cells within. With the help of a digital thermometer, it was easy to control the temperature. Many osteochondral slices were mounted in an agarose structure throughout experiments described herein, and cell viability was not impacted by the agarose gelling procedure, even at temperatures reaching 39°C.

Imaging was sometimes impaired if the osteochondral slices, which were cut by hand, were not flat enough to lay homogenously against the glass bottom surface. Indeed, if different thicknesses of agarose were present between the sample and the glass, this negatively impacted the imaging quality.

Finally, it was possible to reliably label cells within osteochondral slices, while the slices were embedded within the agarose structure. This allowed us to first embed the sample within the agarose, acclimatize the sample to the new diffusion microenvironment, and label the samples thereafter. The procedure of mounting, culturing and labeling was therefore successfully performed throughout the experiments.

4.2 Cell Labelling

4.2.1 Lentiviral vector cell labelling

Using a lentiviral vector to label cells with GFP, the fluorescence in the cells started increasing on day three, post infection. On day five post infection it was very bright (Figure 4.1) and sustained for at least a month. The signal was also sustained after thawing, following explant freezing at -20°C. The cells in explants, including the calcified cartilage, deep zone and subchondral bone, were transduced, as they exhibited a visible GFP signal.

Staining for viability after transduction did not reveal more dead cells than before transduction. This proved that the infection itself did not cause detectable cell death within the explants.

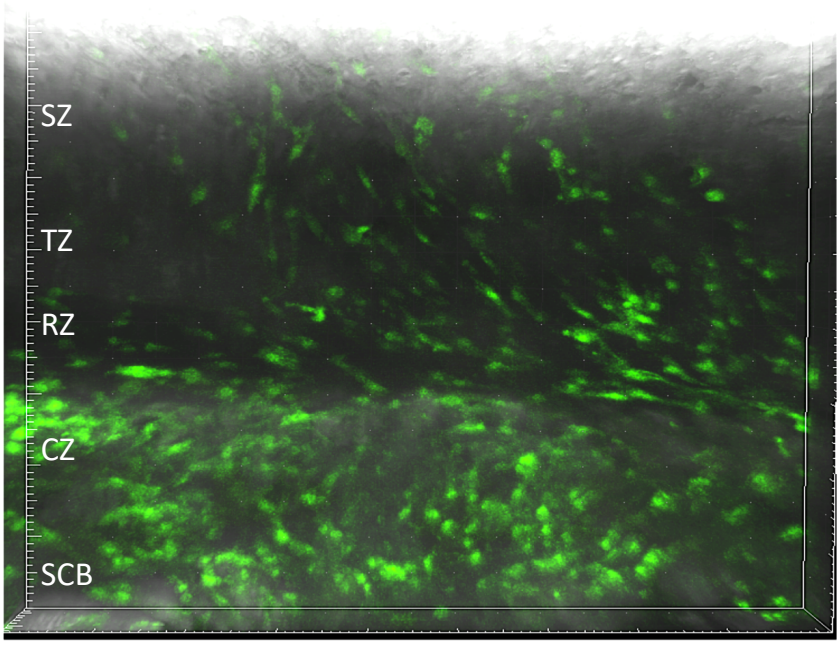

Figure 4.1. Labelling with Lentiviral vector 5 days post transduction (source [1]).

4.2.2 AAV vector cell labelling

With an AAV vector, it took up to three days for the GFP transgene to appear. The GFP transgene signal was brightest at day 3 (Figure 4.2) and fading thereafter. After about 7 days following transduction, no GFP-signal was visible in the explant samples anymore. The fluorescence was not as bright as with the lentiviral transgene, even when the dosage of AAV was increased. The whole cell appeared fluorescent, indicating that GFP was spread throughout the cell, but it was difficult to distinguish in a 3D sample. Also, with this method of labelling, mostly cells in the subchondral bone, the calcified cartilage and the deep zone were transduced. As with the Lentiviral infection, AAV infection did not affect the viability of cells.

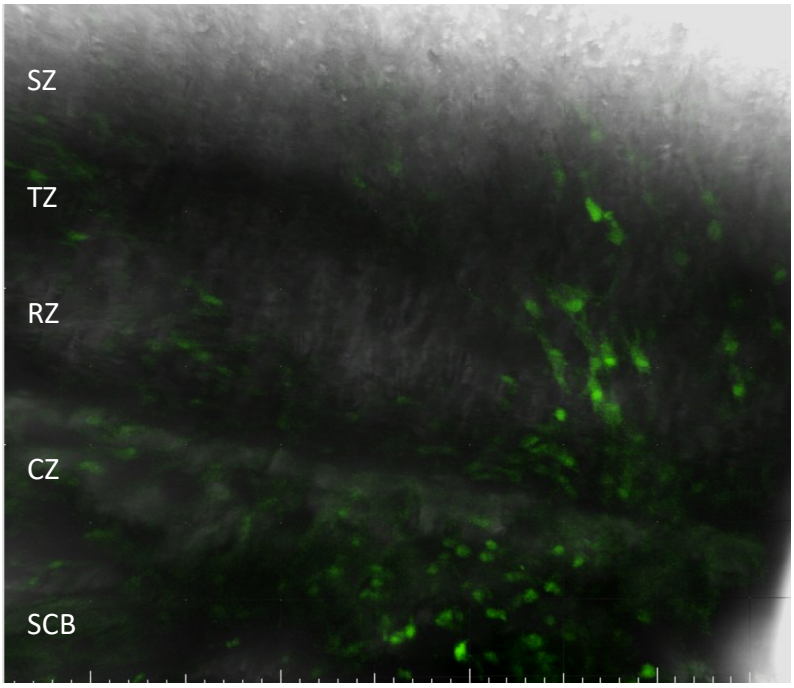

Figure 4.2. Labelling with AAV-vector 3 days post transduction (source [1]).

4.2.3 CMFDA cell labelling

Using the CMFDA cell-membrane labelling, the fluorescent signal was very bright. That was already the case immediately after staining, as is expected when using a passive stain. It was not clear whether the label was localized in the cell membranes only or labelling the whole cell, mainly due to technical limitations with 3D imaging with the CLSM. The stain lasted for a minimum of 14 days in culture and did not have an effect on the viability of cells within explants. In order to label cells within the subchondral bone, the labelling agent would have to penetrate through the bone tissue, which is more challenging than water-filled tissues such as cartilage. By extending the labelling step in the protocol to 24 hours (compared with 40 minutes using the standard protocol), it was also possible to visualize the subchondral bone cells within explants.

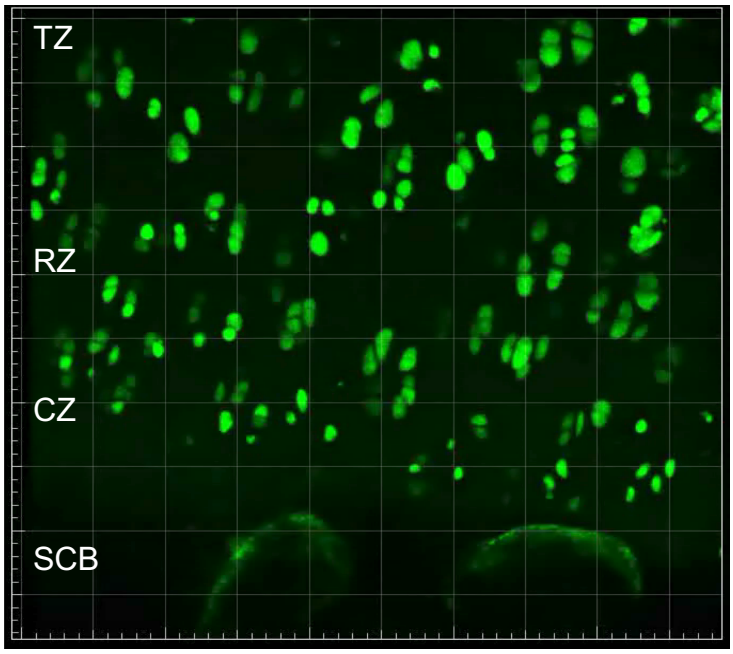

Figure 4.3. Labelling of cells in an osteochondral slice with CMFDA membrane stain.

4.2.4 CMAC Blue cell labelling

This label was chosen in order to explore the possibilities to create multiplex imaging, using for example the Live/Dead labelling as well as a passive membrane stain. The handling of this passive membrane stain was as simple as the CMFDA. Unfortunately, the imaging of cells within the blue emission spectrum was not as good as with the green wavelengths. Indeed, the signal was very weak, especially in 3D tissues. Because of this, this label was not explored any further.

4.2.5 SiR Actin cell labelling

The active SiR Actin cytoskeleton label was very easy to handle. A positive signal indicated both the cell viability as well as active changes in the cytoskeleton. The labeling technique was very reliable and was successful both with free floating samples as well as agarose-embedded samples. After a longer staining procedure, this label also showed the cells in the subchondral bone very clearly. However, the SiR Actin label had to be present in the culture media throughout the experiment, in constant contact with the explants, which may have caused unknown side effects as well as a high usage of the label.

4.2.6 Summary of findings and choice of label for time-lapse experiments

After trying different methods of staining, the AAV was not the first choice, because the transduction took time, was not reliable and the GFP expression disappeared in 7 days. The lentivirus vector worked better, labelling the cells intensively and lasting for much longer. Still, the whole transduction procedure was quite complicated, mainly due to biosafety requirements. Indeed, the explant samples had to be carefully transported to the virology institute, transduced, then transported back to the CABMM laboratory for further processing.

As for the passive membrane label CMFDA CellTracker, it was very easy to handle compared to the viral vectors, and it took only 40 minutes to label the cells, which then exhibited the fluorescent signal immediately after the labeling procedure. In addition, the stain was as visible and long lasting as the lentivirus vector. The CellTracker CMAC Blue was as easy to handle as the CMFDA. Its labelling capability was equivalent, as visible by eye, but was difficult to image at this wavelength in a 3D sample.

The SiR Actin live label, the fluorescent signal was very reliable, worked well, especially in time-lapse experiments and as a great advantage could be combined with other stains as well (the emission spectrum did not overlap with the standard green emission of the Live stain, for example).

Therefore, given the various pros and cons of the labelling methods tested, the SiR Actin was chosen to image samples for further experiments described in this thesis.

4.3 LPS stimulation *in vitro* with healthy explants

Using healthy osteochondral explants from the shoulder joint of sheep sacrificed for other experiments, a stimulation of the explants *in vitro* was attempted using LPS. First, a dose titration was achieved to find the maximal dosage not causing cell death. Thereafter, the stimulation experiment was performed.

4.3.1 LPS dosage and explant viability

Using 2 µg/mL LPS in growth media was a too high dosage, as it killed most of the cells in the explant after 24 hours as well as after 48 hours, as seen in Figure 4.4.

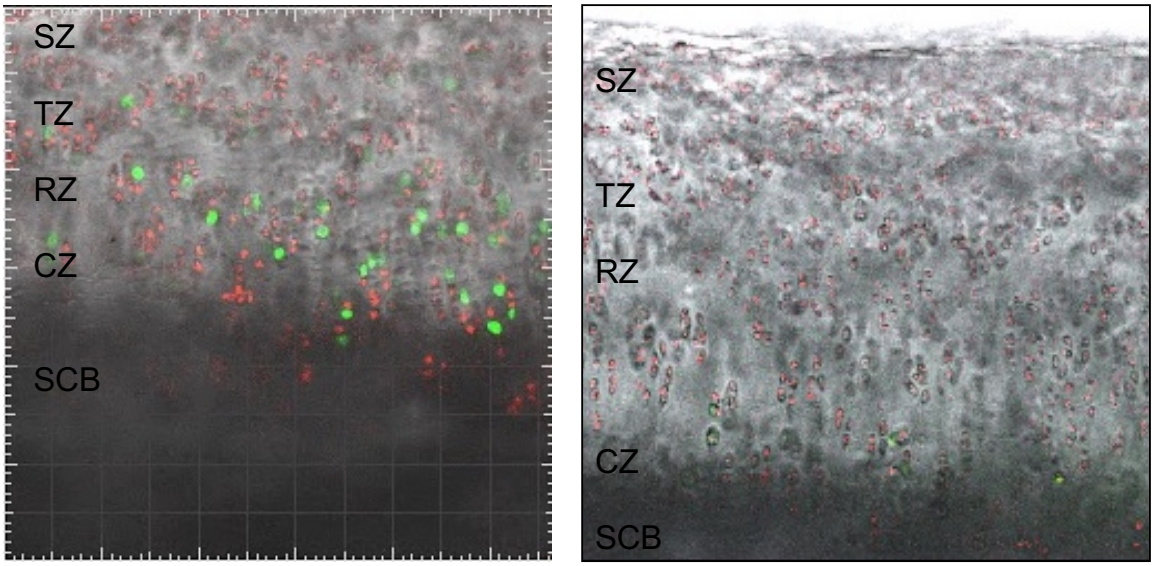

Figure 4.4. Live/Dead staining after 24-hour (left) and 48-hour (right) stimulation with 2µg/mL of LPS.

Using 1 µg/mL LPS, cell death did not occur and there were many viable cells and no more dead cells than what is normally observed in control samples (unstimulated). No visible changes were detected within the first 24 hours (Figure 4.5). After 48 and 72 hours, however, some cluster formation was already visible following LPS stimulation (Figure 4.6). This confirmed that the dose of 1 µg/mL LPS was sufficient enough to cause a cellular effect, but not too high to cause cell death. Therefore, this dose was used in the following LPS-stimulation time-lapse experiment.

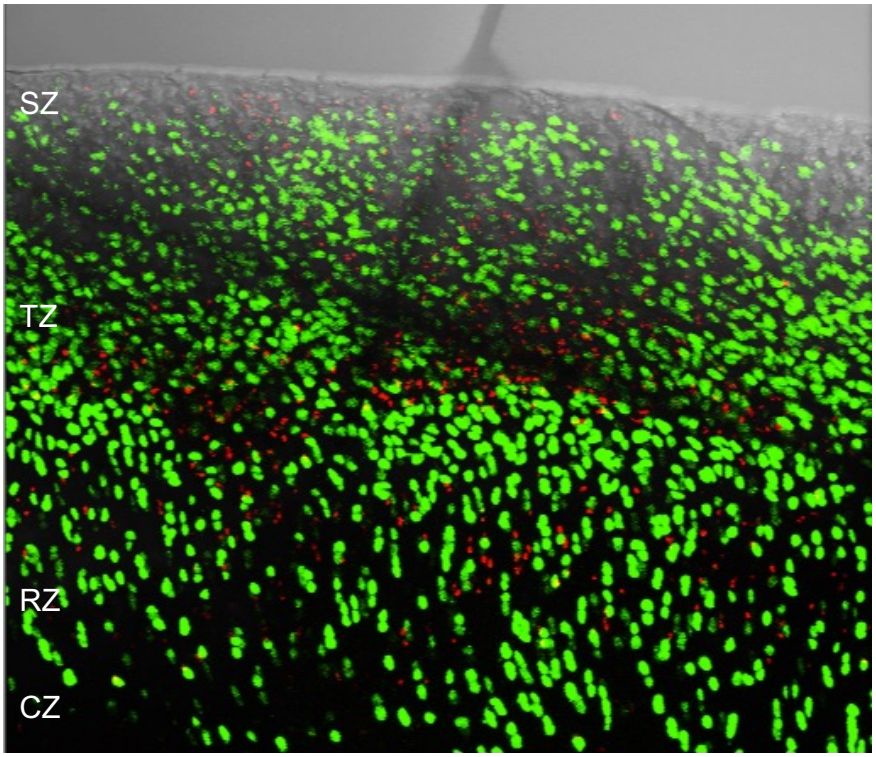

Figure 4.5. Live/Dead staining of stimulated explants with 1µL LPS/mL media after 24hours, showing no changes in cell order and viability.

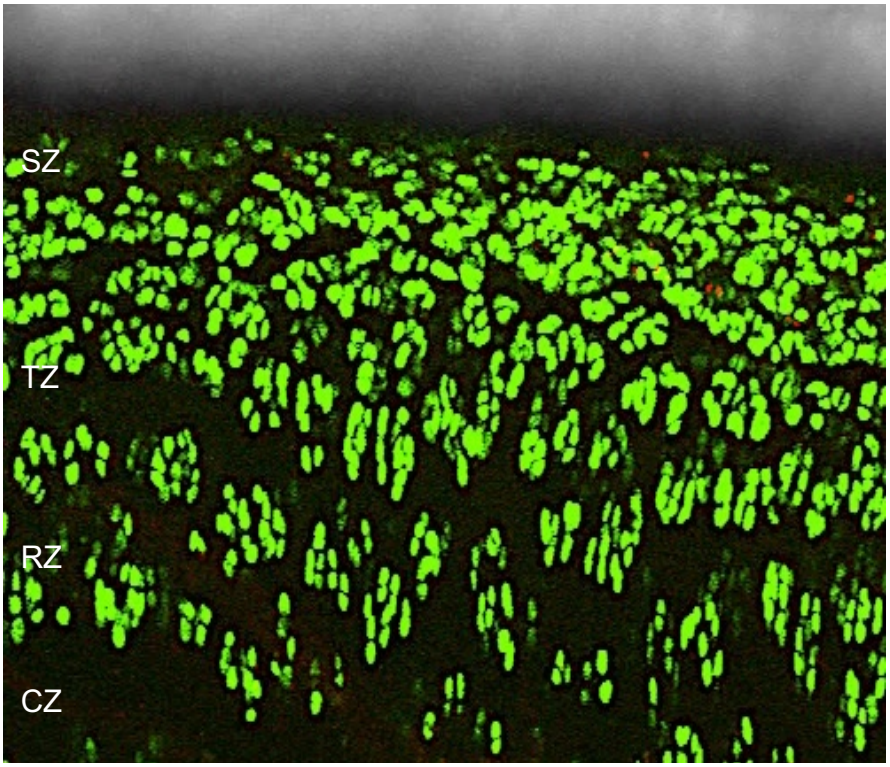

Figure 4.6. Live/Dead staining of stimulated explants with 1µg/mL LPS after 72hours, showing clear cluster formation but hardly dead cells.

4.3.2 Timelapse after LPS stimulation

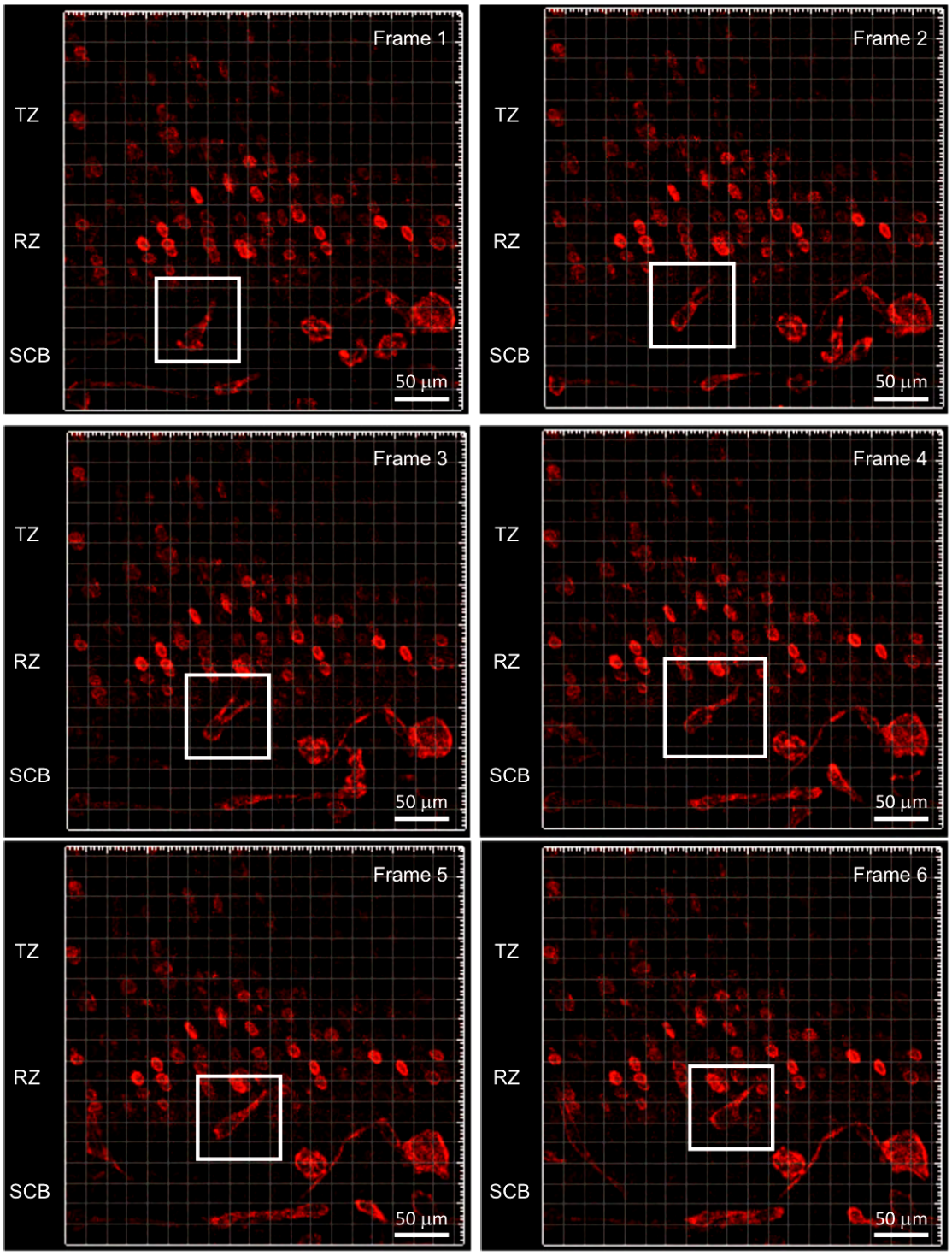

Figure 4.7. Snapshots (Frame 1 through 6) from Group 1 sample time-lapse (10-13 days pre-culture, 7 day LPS stimulation), showing a cell (highlighted in the white frame) from the subchondral bone (SCB) crossing into the calcified cartilage layer (RZ). TZ indicates Transition zone, RZ indicates Radial zone, SCB indicates Subchondral bone zone. The scale bars indicate 50 µm.

While comparing the results of the groups listed in Table 3.4, the highest activity was observed in groups in which explants were cultured for 10-13 days after harvesting. The activity was clearly detectable regardless whether samples were stimulated with LPS or

not. Activity was defined as detected migration behavior and possible proliferation. Both migration from subchondral bone into the overlying articular cartilage as well as migration and suspected proliferation within the cartilage tissue were detected. The LPS group samples, especially the ones with 7 day LPS stimulation, appear to show higher cell activity, however, this was not quantitatively or qualitatively confirmed.

4.4 Imaging of *In vivo* Experiment Explants

Explant samples taken from the two treatment groups were processed in order to perform confocal imaging to detect the Live/Dead labelling as well as time-lapse imaging to detect cell activity, with cells labeled with SiR Actin.

4.4.1 Control Group

The cartilage harvested from the control group animals was expected to show signs of degeneration, as no treatment was applied, following the metaphyseal tibial defect creation, which is known to cause apposing cartilage degeneration. The degeneration was expected to appear directly above the metaphyseal defect area, whereas the cartilage from surrounding areas was expected to be unaffected. The bordering cartilage may exhibit degenerative effects as well, but not as severe as those above the defect zone.

4.4.1.1 Viability test

After harvesting and washing the plugs, a viability check was first performed with a simple LIVE/DEAD staining. Slices were chosen from a plug that was harvested in the defect region. Slices were also chosen from a plug taken on the border of the defect, which had an “in-defect” and a “non-defect” part.

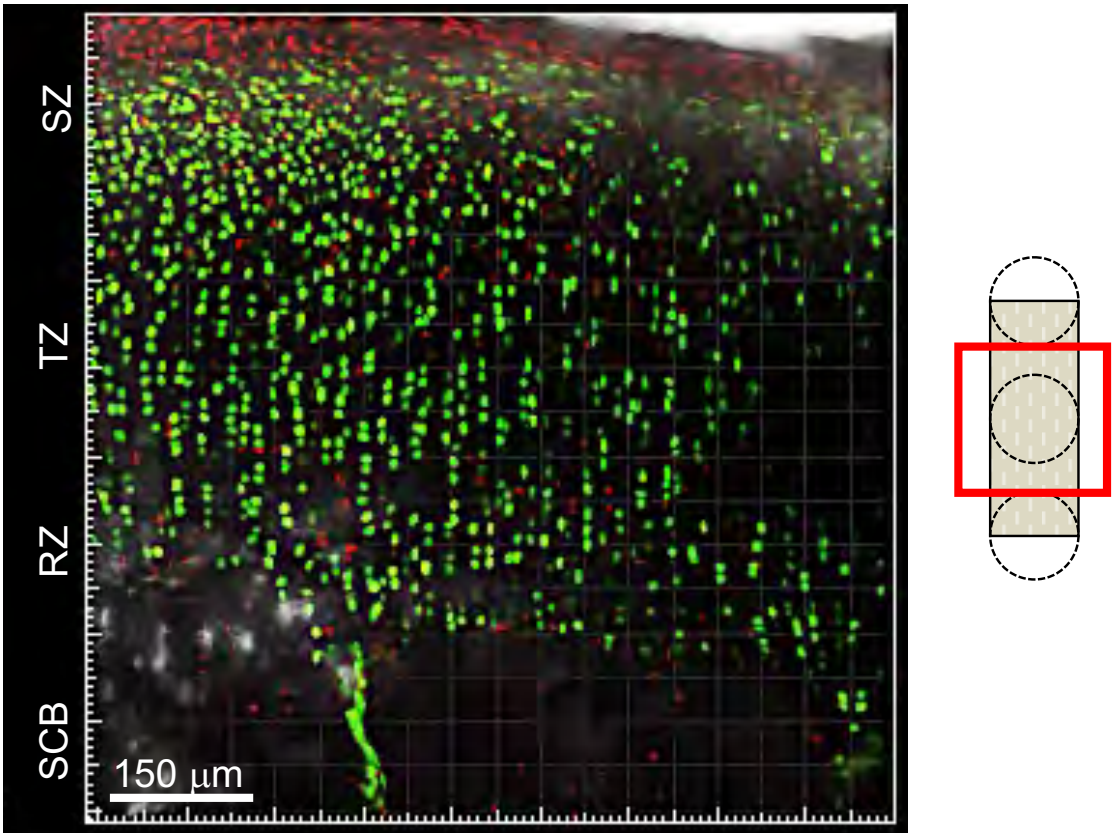

Figure 4.8. Live/Dead staining of control sample harvested above metaphyseal defect, as shown in the schematic on the right. SZ indicates Superficial Zone, TZ indicates Transition zone, RZ indicates Radial zone, SCB indicates Subchondral bone zone. The scale bars indicate 150 µm.

In the samples taken from the defect area, hardly any live cells (green in Figure 4.8) were seen in the subchondral bone, but also very few dead cells (stained red) were seen, indicating that no cells were present in that zone, due to the underlying defect. This could be due to cells migrating out of this area or that cells had died and that DNA was washed (or digested) away at an earlier timepoint *in vivo*, prior to sample harvest. The cells in the transition zone and radial zone were alive, with few dead cells. However, many dead cells were detected in the superficial zone, possibly indicating the degrading health of the cartilage tissue as a whole, in this area above the defect.

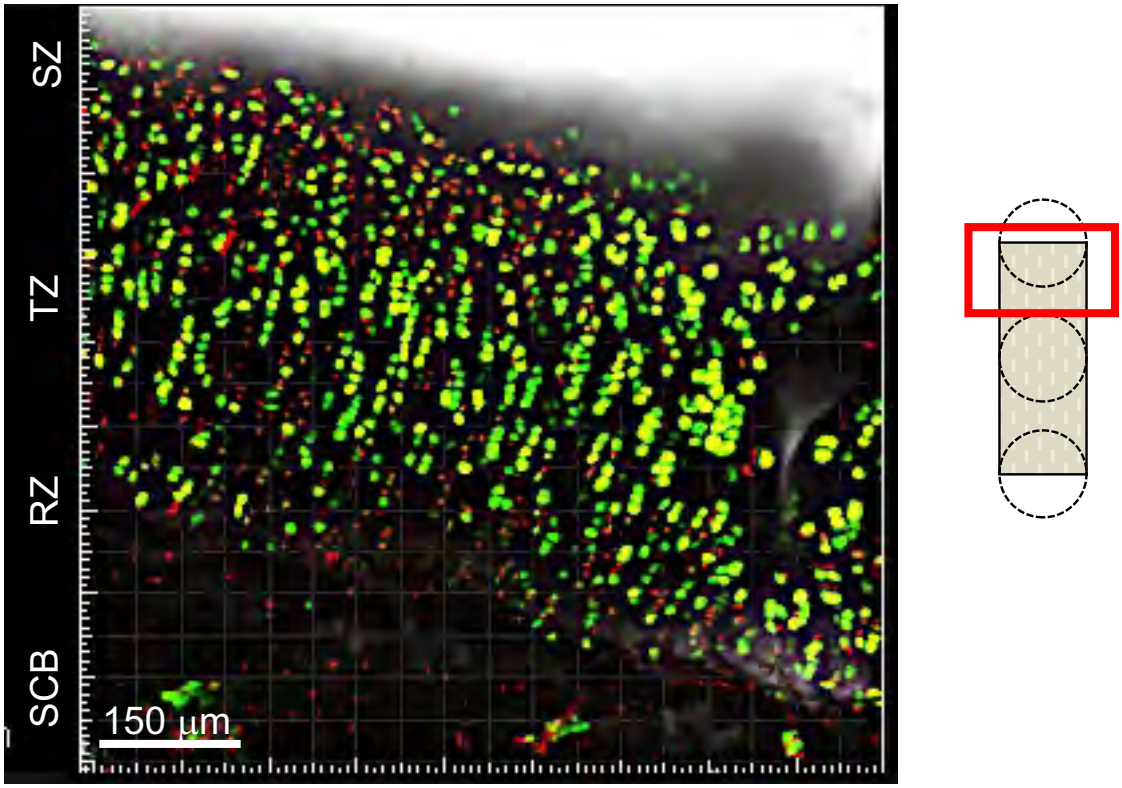

Figure 4.9. Live/Dead staining of control sample harvested on the border, above-defect side, as shown in the schematic on the right. SZ indicates Superficial Zone, TZ indicates Transition zone, RZ indicates Radial zone, SCB indicates Subchondral bone zone. The scale bars indicate 150 µm.

In Figure 4.9 samples taken above the defect area, but on the border of that region, hardly any live cells were observed in the subchondral bone. In this case, however, dead cells were observed in that zone, unlike in Figure 4.8. Regarding the cells in the cartilage layer, about 30% seemed to be dead, with increasing amounts closer to the superficial zone, but less so, however, than in the defect area as in Figure 4.8.

On the "non-defect-side", as seen in Figure 4.10, cells in the subchondral bone were all dead except for very few live ones. However, the cartilage zones looked very viable and hardly showed any dead cells. This was in stark difference to what was observed in Figure 4.8 and in Figure 4.9 and went in line with the expectation that the cartilage tissue above the defect area would exhibit degeneration, but not in areas where there was no underlying bone defect.

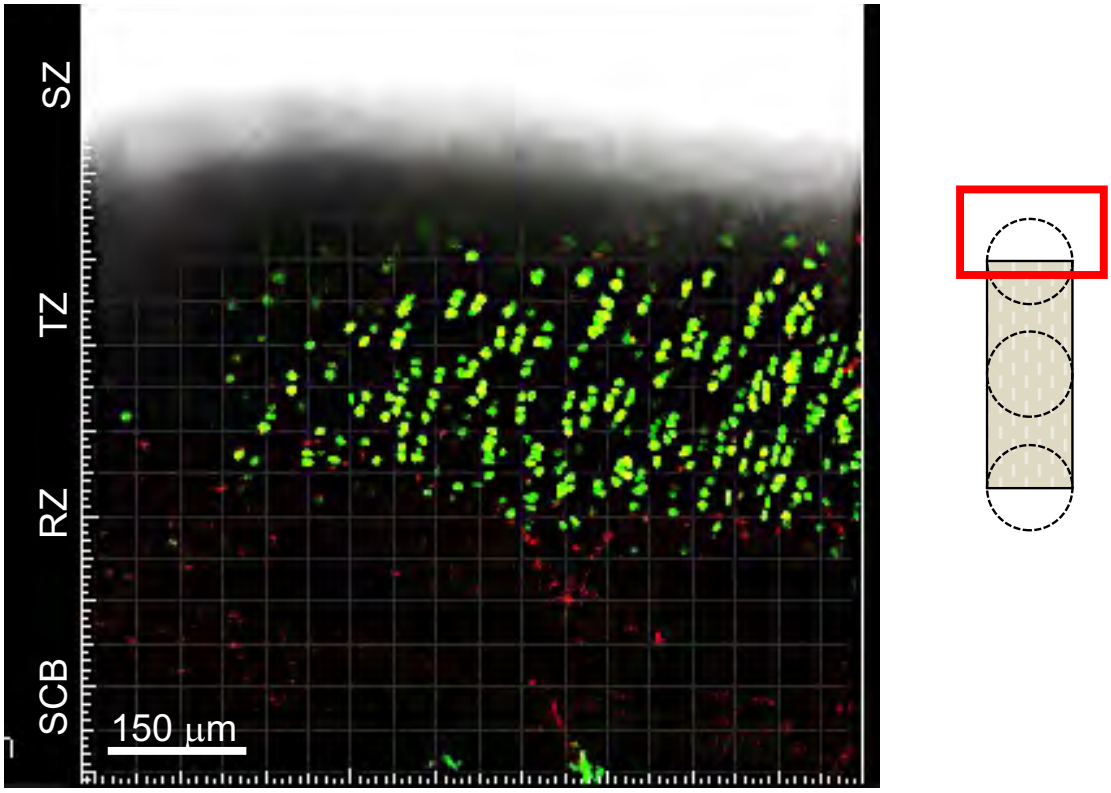

Figure 4.10. Live/Dead staining of control sample harvested on the border, non-defect side, as shown in the schematic on the right. SZ indicates Superficial Zone, TZ indicates Transition zone, RZ indicates Radial zone, SCB indicates Subchondral bone zone. The scale bars indicate 150 µm.

4.4.1.2 Time-lapse

Even though few cells were detected in the subchondral bone using the viability assay, a notable number of cells was detected through the time-lapse imaging of SiR Actin labelled cells. This may be due to the SiR Actin label diffusing differently within bone than the viability assay labels. While no clear migration of cells from subchondral bone into the overlying hyaline cartilage could be noted within the time frame of 72 hours, subchondral bone cells nevertheless did not remain static in the frame of view. Instead, the visible cells in the subchondral bone seemed to move in the z-axis, coming into the frame of view (Frame 2 of Figure 4.11) and then back out (Frame 4 of Figure 4.11). Furthermore, the labelled subchondral bone cells seemed to aggregate in clumps in the subchondral bone tissue, which may be an indication of abnormal behavior for these cells. As for cells within the cartilage zones, few were detectable in the time-lapse. This was likely a combination of technical imaging difficulties and the presence of many dead cells within the cartilage layer, as shown in the viability assay of such samples. This combined challenge made it difficult to evaluate any changes within cartilage cell populations.

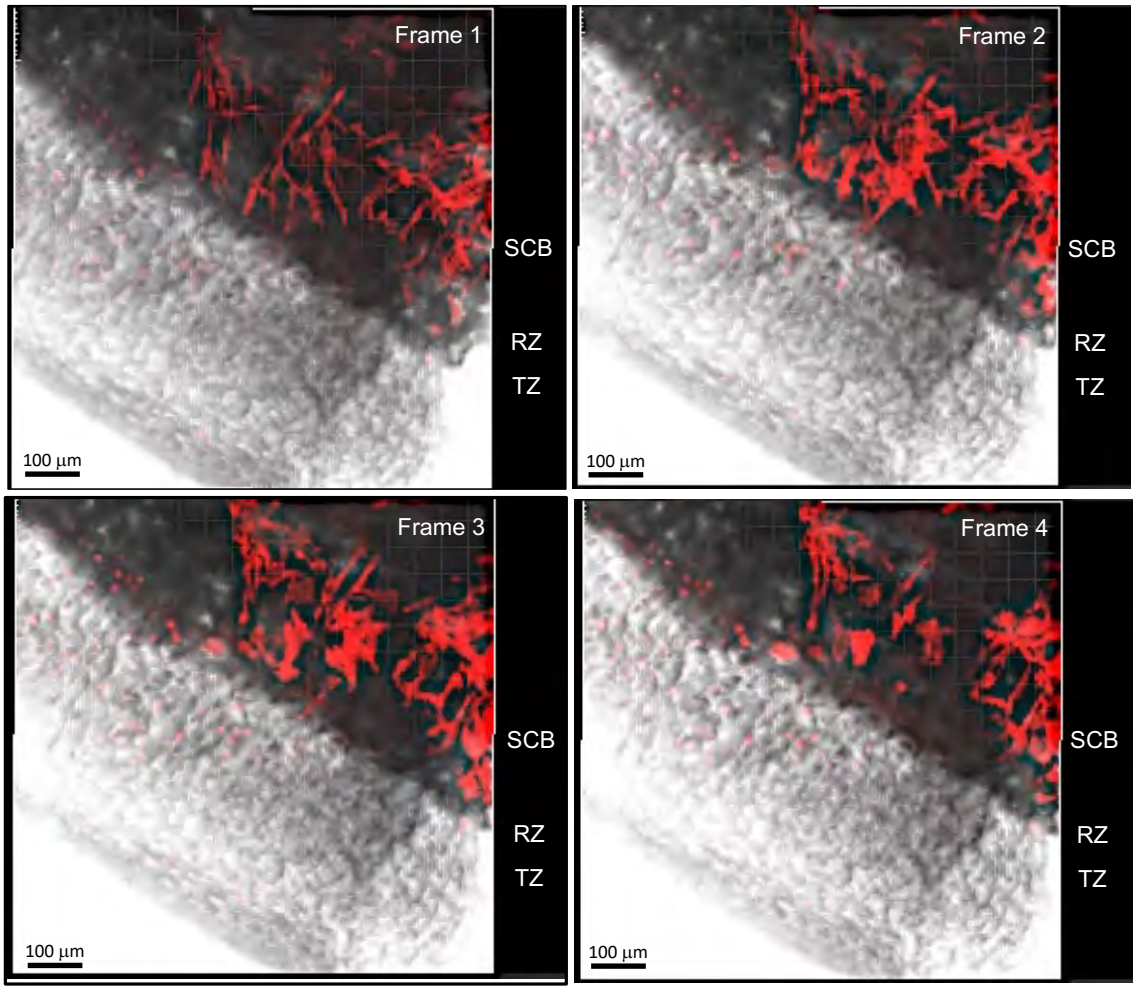

Figure 4.11. Serial snapshots (Frames 1 through 4) taken from the time-lapse of a control-group (untreated with Diclofenac) sample. Cells were labelled ex-vivo with SiR Actin. TZ indicates Transition zone, RZ indicates Radial zone, SCB indicates Subchondral bone zone. The scale bars indicate 100 µm.

4.4.2 Diclofenac-treated Group

The cartilage from the samples harvested from the Diclofenac-treated group was expected to benefit from the anti-inflammatory treatment, despite the metaphyseal defect creation.

4.4.2.1 Viability test

Viability assays were performed on the harvested osteochondral explants from sheep stifle joints, treated with Diclofenac every day for a total of 14 days through a TDA system. Slices taken from explants extracted within the defect area (Figure 4.12) showed few labelled cells in the subchondral bone. Some dead cells were detected in this layer. The cells in the cartilage layer, however, were very strongly labelled and were viable with only very few scattered dead cells. This was in contrast to control-group slices, in which superficial cartilage cells were not viable (Figure 4.8). The same pattern was observed on the edge of the defect, both with the "in-defect" half (Figure 4.13) and the "non-defect"

half (Figure 4.14). The “in-defect” half showed a few more dead cells and the live cell signal was overall weaker.

4.4.2.2 Time-lapse

The time-lapse imaging of Diclofenac-treated samples revealed the number and location of labelled cartilage cells was physiological. No clear changes were detectable in the cartilage layers throughout the time-lapse duration. In contrast, a great number of subchondral bone cells were detected and increase throughout the time-lapse imaging window. This indicated either a proliferation of subchondral bone cells or a migration of subchondral bone cells into the field of view or a combination. The discrepancy between the subchondral labelling in the viability assay and using the SiR Actin was further confirmed with the samples from the Diclofenac group. Subchondral bone cells did not form clumps or non-physiological aggregates, as in the control group, but instead seemed to migrate into the cartilage layer. The migration pattern was however not unidirectional.

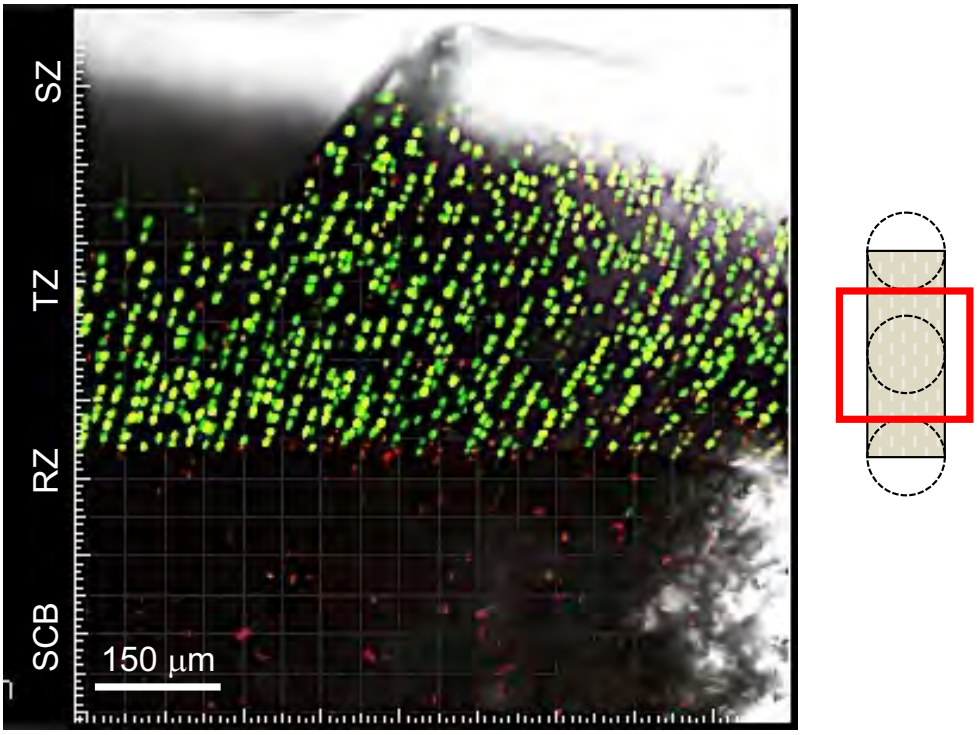

Figure 4.12. Live/Dead staining of Diclofenac-treatred sample harvested above metaphyseal defect, as shown in the schematic on the right. TZ indicates Transition zone, RZ indicates Radial zone, SCB indicates Subchondral bone zone. The scale bars indicate 150 µm.

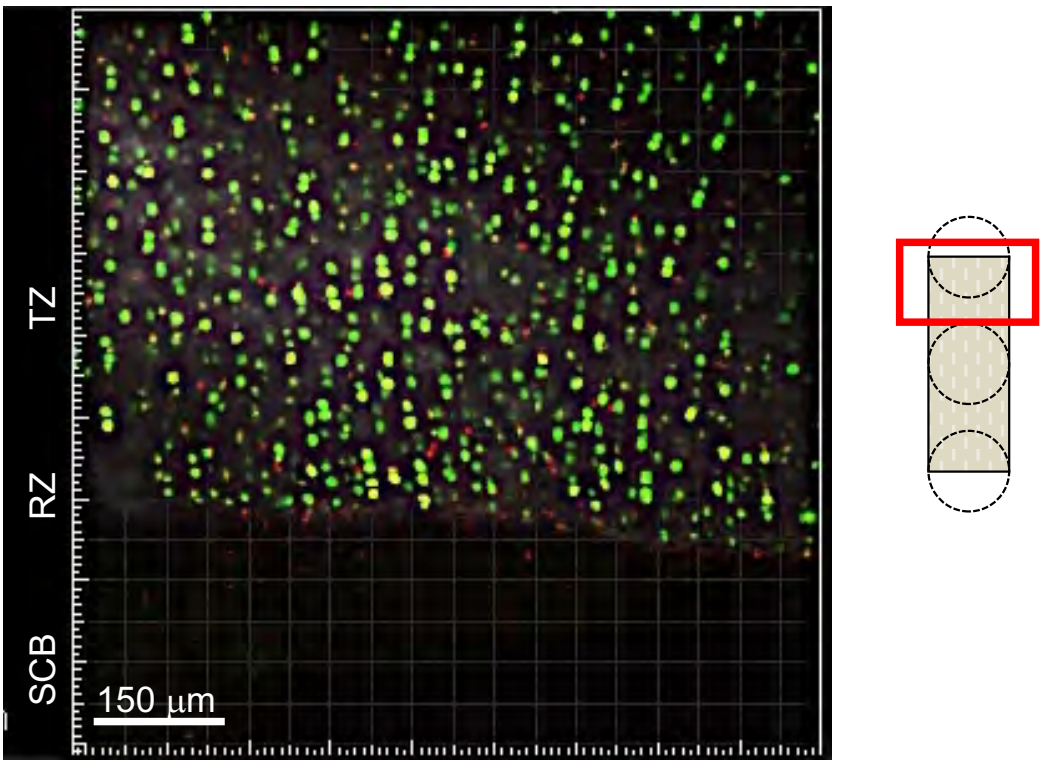

Figure 4.13. Live/Dead staining of Diclofenac-treated sample harvested on the border, above-defect side, as shown in the schematic on the right. TZ indicates Transition zone, RZ indicates Radial zone, SCB indicates Subchondral bone zone. The scale bars indicate 150 µm.

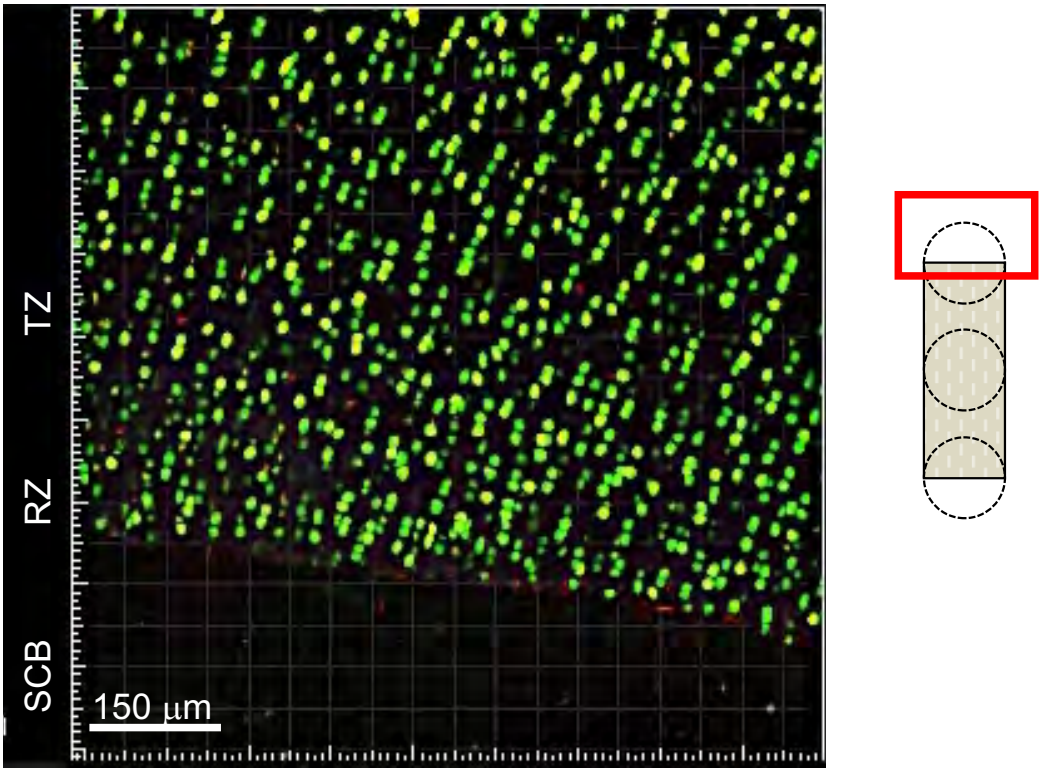

Figure 4.14. Live/Dead staining of Diclofenac-treated sample harvested on the border, non-defect side, as shown in the schematic on the right. TZ indicates Transition zone, RZ indicates Radial zone, SCB indicates Subchondral bone zone. The scale bars indicate 150 µm.

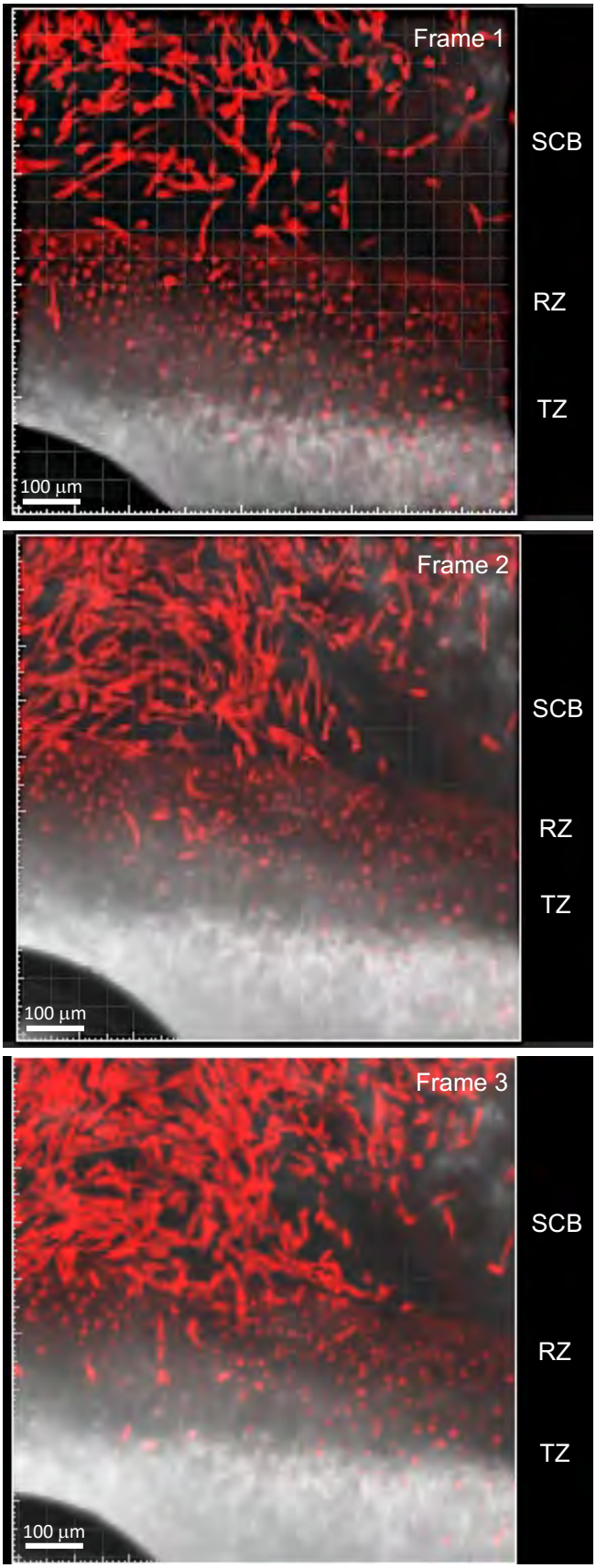

Figure 4.15. Serial snapshots (Frames 1 through 3) taken from the time-lapse of a Diclofenac-treated sample. Cells were labelled ex-vivo with SiR Actin. TZ indicates Transition zone, RZ indicates Radial zone, SCB indicates Subchondral bone zone. The scale bars indicate 100 µm.

5 Discussion

In summary, this thesis describes the successful design of a functioning system to track cells in osteochondral explants of sheep *in vitro*.

With this technique, the microenvironment of the cells was successfully maintained, even with cell labelling techniques used. We managed to stain cells in cartilage and bone tissue and proved that the cells were viable in the calcified layer. The described cell culture method made it possible to keep explant samples viable in culture for up to 8 weeks, both as slices and as whole osteochondral plugs. The osteochondral interface was therefore preserved *in vitro* and the cells in this region could then be observed and tracked over 72 hours. Explants in culture could also be stimulated with soluble factors, simulating inflammation. Furthermore, it was also demonstrated that viral vectors using AAV and lentivirus could transfect cells in the subchondral and chondral part of the osteochondral slices. With all techniques it could be verified that cells of the calfied cartilage zone were viable and not hypertrophic. To the knowledge of the author, these findings were never reported in the literature.

5.1 Agarose wells / osteochondral slices / culture

The OATS technique of explant harvesting, as well as the processing and culture with the described media worked very well with no instances of contamination throughout the experiments.

As for the immobilization technique with the agarose structures, roughening the well walls with sand paper was the most successful method to maintain the agarose structures static. However, square wells would completely prevent the movement of the agarose structures. Square wells were not commercially available and may need to be custom designed and produced for this purpose.

As for the osteochondral slices, it was not always possible to guarantee that the samples lay flat on the glass-bottom of the well. That is because the explant slices were cut by hand and in consequence many were curved or uneven on a microscopic level. This could cause the agarose to penetrate between the sample and the glass-bottom, which changed the focus while imaging. Developing a standardized tool to slice the explants evenly would be ideal, in order to reliably create flat surface explant slices and slices of similar thicknesses. Such a cutting tool would, however, need to be very sharp in order to

preserve the viability of the cells within the explants. Indeed, blunt tools could easily crush the cells and compromise the viability of the samples during preparation.

Finally, the agarose structure created here in order to immobilize the samples for imaging may still be vastly improved. For instance, the use of a different, biocompatible material may provide an advantage to agarose, especially if that new material is both stiffer and less permeable than agarose. Ideally, completely separating the chondral and bone parts would allow the exposure of both tissues to different growth media formulations with different stimulating factors simultaneously. This would better mimic the situation in the native tissue.

5.2 Labels

With the present study, we were able to develop techniques to label cells within osteochondral explants. Most cell labels are designed to be used on cell cultures or cell suspensions, and not on tissue cultures. Our experiments showed that osteochondral tissues, notoriously difficult to label because of the dense tissue structure, were successfully labelled using various methods. Furthermore, the osteochondral explants could be labelled while embedded in the agarose structure.

As the aim of this thesis was to investigate migration of different cell types within the osteochondral tissue, having a cell-specific live label would have been ideal. However, there was no chondrocyte-specific or bone-cell specific live cell label available on the market. We therefore had to explore several techniques to label live cells within a tissue, regardless of the cell type. The label needed should not affect the viability of the tissue and should successfully label all cells in cartilage as well as in subchondral bone over a selected time period (at least 7 days).

The CMFDA CellTracker green stain turned out to be a very “easy-to-do” stain, which colored the chondrocytes with great success. Being a passive membrane stain, it was not expected to interfere with any normal cell function. However, no matter how the protocol was modified, there was no way for it to stain the cells in subchondral bone.

Both viral vectors worked in labelling cells throughout the explant slices. The lentivirus-infected cells exhibited the GFP label 5 days after infection, while the AAV-infected cells exhibited the signal after 3 days but faded completely in the following 4 days. The AAV technique limited the signal intensity as well as the window of imaging to barely 72 hours. With both infection methods, it was not possible to verify the viability of the cells within the explants after GFP expression, or whether the GFP expression was sustained over

time, as opposed to GFP simply being deposited and the cells subsequently dying. This latter possibility was suspected after the GFP signal was detected following the freezing of samples at -20°C. In this case, the cells would not be expected to survive the freezing process, but the GFP signal was still visible. The link between a viable cell and a visible GFP signal was therefore not always verifiable. Having a transgene, which emits at a different wavelength than the viability stain, would be ideal.

The SiR Actin stain was definitely the best option because it stained the cells localized in subchondral bone as well as in cartilage and additionally was able to show the dynamics of the cytoskeleton in each cell. This was not only an indirect proof of viability, but also showed how cells changed their skeleton in order to migrate. A negative aspect regarding this stain, was that it could possibly influence the cells over a long time period. Because it was necessary to include it in the standard culture media in order to maintain the signal, cytotoxicity may be possible, even if we could not detect it. The SiR Actin label was tested on human fibroblasts in culture, as described by the manufacturer, and no cytotoxic effect was observed within 24hours[71]. A study of how continuous SiR Actin exposure to cells within cultured tissues would be necessary to ensure no adverse effects.

Finally, the viability assay label was a useful tool to verify the viability of the cells within the explants. However, this was only possible within the cartilage layer, as we suspected the diffusion of the label within the subchondral bone to be limited. The use of an alternative viability label, or an adapted penetration protocol, would be needed, especially in order to show the viability of the subchondral bone.

Rating	Lentiviral vector	CMFDA	SiR Actin	AAV vector
+	+ Long lasting + Strong signal	+ Quick and easy + Bright + Passive	+ Easy + Stains well + Bone cells + Stains viable cells only	+ Safer than lentivirus + Low risk of insertional mutagenesis
–	- Uneasy handling - Safety (BSL2) - Risk of insertional mutagenesis - Cannot simultaneously check viability	- No bone cells were stained - cannot simultaneously check viability	- possible cytotoxicity	- Uneasy handling - Fades after 7 days - Not very bright

Table 5.1. Positive and negative aspects of the used labelling methods.

5.3 Time-lapse

The time-lapse experiments were performed to prove migration of cells from the subchondral bone tissue into the overlying hyaline articular cartilage. This was tested in healthy osteochondral explants from sheep cadavers as well as explants from sheep stifles following a surgical procedure, which is designed to compromise cartilage viability.

In order to answer the scientific question, namely whether anti-inflammatory therapy stimulates cells within osteochondral tissues, the establishment of the imaging technology was needed. To that end, we were able to successfully maintain osteochondral explant slices in culture, embedded in agarose structures while labelling the cells within throughout an imaging period of 72 hours. This was achieved in various samples and the imaging protocol was adapted throughout the experiments to ensure the capture of labelled cells within the 3D tissue. This included the setup of automated z-stack imaging as well as automated pre-defined regions of interest across 12 different slices positioned in 6 different wells. After much adaptation, the samples were successfully immobilized throughout the imaging period. Imaging the fluorescent signal was combined with a brightfield image in order to identify the different layers of osteochondral tissue within each sample. However, despite the successful imaging, showing the migration of cells in explants still proved to be a technical challenge, which made the reliable comparison between treatments difficult to achieve.

Due to the fact that the cell culture media needs to be changed every 72 hours in order to guarantee the viability, the duration of the time-lapses was also limited to 72 hours. If it were possible to somehow change the media during the time-lapse, perhaps in an automated way, and given the observed dynamics of the cells, imaging over twice the current time window would be recommended. A longer time frame is needed because the cells within a dense tissue structure such as the osteochondral tissue likely require a longer time to migrate than cells on tissue culture plastic. In addition, due to the very dense tissue composition, cells would move very slowly, which is the reason why the interval of recordings should not be less than 1 hour. This creates an advantage when imaging of multiple days because it reduces the imaging file size and the exposure of the samples to the laser. Different labelling methods would react differently to laser exposure, with CMFDA being the most vulnerable to bleaching because it is a passive membrane stain. The SiR Actin would only be mildly affected by bleaching as it is continuously present in the media in an inactive form. Finally, the method using expressed transgenes

(Lentivirus or AAV infection), would be the least affected, because "fresh" GFP is constantly produced by the cells.

In all time-lapse recordings, a clear activity and cell movement was shown in the subchondral bone, especially in the Diclofenac-treated group. This was also the case in the cartilage layers where more activity was visible in samples treated with LPS. In this case, a directional movement from subchondral bone into the above lying cartilage could be detected. This also showed that the believed impenetrable border between subchondral bone and cartilage could be penetrable and that these two tissues would be able to communicate. From a theoretical point of view, there is evidence supporting this observation, especially when taking into account the vessels reaching into the calcified cartilage layer from the subchondral bone. Previous studies have also shown there is a clear change in subchondral bone due to cartilage defects or degeneration. A "cross-talk" has been clearly described between these adjacent tissues.

Based on our experimental evidence, it is not yet clear if all the cells move within the sample, if only a subset of cells move, or if the movement has a preferential direction. In the case of the Diclofenac-treated sample, in which a high cell movement and activity was observed, the cells may have in fact migrated out of the tissue and may have been proliferating outside the explant. Because imaging the 3D tissue was challenging, it was not possible to determine where the cells were migrating in relation to the sample edge. Still we could prove the viability of these cells and the cells in the deep and calcified cartilage layer.

5.4 *In vitro* inflammatory challenge

In order to give the cells a "reason" to migrate or proliferate we decided to add inflammatory factors to stimulate them through the cell culture media. LPS is one of the most effective endotoxins inducing inflammation. LPS is often used in research and, depending on the dosage, it is either cell toxic or stimulating regarding cell proliferation[60]. We determined a not cytotoxic dosage before setting up the experiment. We also quickly realized that it would take more than 24 hours to cause an effect, such as movement or proliferation. This could be because of the dense tissue we were working with or because of the cell type or both. Based on our experimental evidence, the highest effect was visible after a 4 to 7 day LPS stimulation.

LPS has been described to accelerate changes within cultured tissues. An additional stimulation with other inflammatory factors (e.g. TNF-α or Il-1-β) or a cocktail would be

interesting to investigate as well. It is not yet known what would be the ideal stimulant, which would create an inflammatory situation *in vitro* around a osteochondral explant.

5.5 *In vivo* experiments

Regarding the viability tests in the control group, a subchondral bone defect clearly had an influence on cell viability in the cartilage layers, as well as on the surrounding subchondral bone cells. The cartilage cells above the defect were much less viable than ones outside the defect, although these cells would likely degenerate sooner or later as well, because the cells in subchondral bone were mostly dead.

The technology developed in this thesis could be used to answer the question why cartilage, e.g. in patients with osteoarthritis, does not remodel. In controls without any treatment after setting the defect, the overlying cartilage is severely degenerated already after 14 days. In the group that was treated with Diclofenac the overlying cartilage was less degenerated and more viable cells were visible, even though cells in the subchondral bone were dead. It may be speculated that, in this case, the cartilage overlying the subchondral bone defect was protected, on one hand through increased proliferation of chondrocytes due to oxygen application and, on the other hand, degeneration of cartilage was decelerated by the TDA treatment with Diclofenac. The latter is a non-steroidal anti-inflammatory drug that is known to decrease the activity of matrix metalloproteinases, which are responsible for matrix degeneration. If the cartilage can be protected and homeostasis maintained through a balance of proliferation and degeneration, cartilage may have the ability to remodel. Results of the Diclofenac group in comparison to the untreated control group suggest this possibility.

Perhaps there was no visible migration from subchondral bone into the cartilage layer because the cells, which usually migrate (namely, the stem cells), seem to be absent due to the created bone defect. It seems that in this short postsurgical period the cells within the subchondral bone could not recuperate yet. In another study of our group using the same animal model, it was demonstrated that the incorporation of intravital fluorescence dye was severely hampered in the subchondral bone area within the first month after creating the defect in the subchondral bone (publication in preparation: doctorate thesis Joya Kaserer). Therefore, if the in-life period were longer than 14 days post-surgery, the cartilage degeneration would likely proceed and the tissue would completely degenerate and cause osteoarthritis. This may be an explanation why the hyaline cartilage

consistently degenerates after fractures of the tibia plateau, although perfect alignment of the fragments was achieved during fracture repair.

The notably viable cartilage cells in the Diclofenac group samples suggest that the anti-inflammatory Diclofenac protected the cartilage with the help of oxygen and deceleration of the cartilage degeneration. This was the case even though the subchondral bone could not remodel. Theoretically the cells, which would migrate into the affected cartilage area, would have to come from adjacent tissue, because the cells in the defect area were damaged in surgery. The Diclofenac-treated cartilage, in comparison to the untreated control group, was clearly more viable. It is very possible that the migration process increases if Diclofenac treatments were administered longer than 14 days post-surgery.

5.6 Conclusion and Perspectives

Creating the first functioning system, which allows to track cells in an osteochondral explant tissue culture, describing bone and cartilage as a unit, is an immense progress in cartilage research. There are endless amounts of research done on bone and cartilage as two separate systems, but in the least cases they are looked at as one unit, although their origin and development is the same or very similar. We were able to not only look at the tissue as a unit, but also track the cells within while maintaining their microenvironments. There may still be technical improvements to achieve, but the described findings in this thesis mark an important step towards osteochondral cell imaging.

The time-lapse experiments have clearly shown migration of cells to be possible, especially from the subchondral bone layer into the calcified cartilage layer. While the differences between treatment groups could not be clearly described due to technical limitations and variability, the developed system is a powerful method to investigate osteochondral tissue migration. Furthermore, the imaging experiments showed that cells in the calcified layer and transition zone, often assumed to be hypertrophic and terminal, were in fact viable and often active.

Further development of this system could be used to reliably prove that cells migrate between these bone and cartilage. Any defect caused to the subchondral bone layer could therefore be linked, on a cellular level, to a degeneration of the overlying cartilage. This would be an additional proof that cartilage and bone act as one unit.

Regarding the migration, it is still unknown how the cells free their path in order to migrate within this dense tissue. Would they have macrophage-like characteristics, or would they break down the tissue and leave by-products? If so, it is questionable what

would happen with the accruing by-products? Also affecting the overall integrity of the tissue would be possible. Are the cells capable of creating their surrounding tissue after "digging" their way to the cartilage layer with help of the by-products, or do they just leave a hollow space behind?

What is also not known is what kind of cells would respond to stimulation: mesenchymal stem cells, which hypothetically differentiate after migrating through the calcified cartilage zone into chondroblasts, resp. chondrocytes? Future studies should definitely address these issues.

Finally, one must not forget that these studies were performed in a sheep model. Although not exactly identical with human cartilage, the basic morphology of sheep is very similar in human beings. Therefore, it may be safely assumed that the basic mechanisms of cartilage remodeling in sheep and humans are similar and much can be extrapolated from these findings.

There are still a lot of unturned stones on the long research-path of cartilage remodeling. But, this work gives us a first stepping stone into the right direction, with a new powerful tool of investigation. Proving that cartilage is supplied with cells from the subchondral bone also in healthy hyaline cartilage would be revolutionary and an important discovery for the future of medicine. It may not only change future therapy of cartilage defects, but also could influence measures of preventing osteoarthritis.

6 Bibliography

1. Schöberl S: Etablierung eines in vitro Organmodells zur Untersuchung der Knorpelremodellierung. Inaugural-Dissertation: Vetsuisse Fakultät Universität Zürich, 2016.
2. Ding C, Cicuttini F, Jones G: Tibial subchondral bone size and knee cartilage defects: relevance to knee osteoarthritis. Osteoarthritis Cartilage 15:479-486, 2007.
3. Day JS, Ding M, van der Linden JC, et al: A decreased subchondral trabecular bone tissue elastic modulus is associated with pre-arthritic cartilage damage. J Orthop Res 19:914-918, 2001.
4. Madry H, van Dijk CN, Mueller-Gerbl M: The basic science of the subchondral bone. Knee Surg Sports Traumatol Arthrosc 18:419-433, 2010.
5. Little CB, Smith MM, Cake MA, et al: The OARSI histopathology initiative - recommendations for histological assessments of osteoarthritis in sheep and goats. Osteoarthritis Cartilage 18 Suppl 3:S80-92, 2010.
6. Gerber C, Meyer DC, Fluck M, et al: Anabolic Steroids Reduce Muscle Degeneration Associated With Rotator Cuff Tendon Release in Sheep. Am J Sports Med 43:2393-2400, 2015.
7. Richter H, Plecko M, Andermatt D, et al: Dynamization at the near cortex in locking plate osteosynthesis by means of dynamic locking screws: an experimental study of transverse tibial osteotomies in sheep. J Bone Joint Surg Am 97:208-215, 2015.
8. Sidler M, Fouche N, Meth I, et al: Preliminary study on carprofen concentration measurements after transcutaneous treatment with Vetdrop(R) in a microfracture joint defect model in sheep. BMC Vet Res 10:268, 2014.
9. Stubinger S, Drechsler A, Burki A, et al: Titanium and hydroxyapatite coating of polyetheretherketone and carbon fiber-reinforced polyetheretherketone: A pilot study in sheep. J Biomed Mater Res B Appl Biomater, 2015.
10. Stubinger S, Nuss K, Burki A, et al: Osseointegration of titanium implants functionalised with phosphoserine-tethered poly(epsilon-lysine) dendrons: a comparative study with traditional surface treatments in sheep. J Mater Sci Mater Med 26:87, 2015.
11. Frisbie DD, Cross MW, McIlwraith CW: A comparative study of articular cartilage thickness in the stifle of animal species used in human pre-clinical studies compared to articular cartilage thickness in the human knee. Vet Comp Orthop Traumatol 19:142-146, 2006.
12. Turner AS: Animal models of osteoporosis--necessity and limitations. Eur Cell Mater 1:66-81, 2001.
13. Cook JL, Hung CT, Kuroki K, et al: Animal models of cartilage repair. Bone Joint Res 3:89-94, 2014.
14. Theodor H. Schiebler WS: Stützgewebe, in Anatomie: Zytologie, Histologie, Entwicklungsgeschichte, makroskopische und mikroskopische Anatomie des Menschen, Vol Springer-Verlag Berlin Heidelberg GmbH, 1991, p 59.
15. Buckwalter JA: Articular cartilage. Instr Course Lect 32:349-370, 1983.
16. Stockwell RA: The cell density of human articular and costal cartilage. J Anat 101:753-763, 1967.
17. Archer CW, Francis-West P: The chondrocyte. Int J Biochem Cell Biol 35:401-404, 2003.

18. Frisbie DD: Synovial Joint Biology and Pathobiology.1096-1114, 2012.
19. Benjamin M, Archer CW, Ralphs JR: Cytoskeleton of cartilage cells. Microsc Res Tech 28:372-377, 1994.
20. Trickey WR, Vail TP, Guilak F: The role of the cytoskeleton in the viscoelastic properties of human articular chondrocytes. J Orthop Res 22:131-139, 2004.
21. Kurosaka S, Kashina A: Cell biology of embryonic migration. Birth Defects Res C Embryo Today 84:102-122, 2008.
22. Small JV, Kaverina I, Krylyshkina O, et al: Cytoskeleton cross-talk during cell motility. FEBS Lett 452:96-99, 1999.
23. B.Hunziker E: <Articular Cartilage Structure in Humans and Experimental Animals. Articular Cartilage and Osteoarthritis 1992.
24. I.V.Knets: Adaption and Remodelling of Articular Cartilage and Bone Tissue, in Helminen HJ, Kiviranta I, Tammi M, et al (eds): Joint Loading, Vol. Bristol, Butterworth & Co. Ltd, pp 251-255.
25. Weiss C, Rosenberg L, Helfet AJ: An ultrastructural study of normal young adult human articular cartilage. J Bone Joint Surg Am 50:663-674, 1968.
26. Seol DR: Chondrogenic progenitor cell response to cartilage injury and its application for cartilage repair. 2011.
27. Lane LB, Bullough PG: Age-related changes in the thickness of the calcified zone and the number of tidemarks in adult human articular cartilage. J Bone Joint Surg Br 62:372-375, 1980.
28. Sophia Fox AJ, Bedi A, Rodeo SA: The basic science of articular cartilage: structure, composition, and function. Sports Health 1:461-468, 2009.
29. Clark JM, Huber JD: The structure of the human subchondral plate. J Bone Joint Surg Br 72:866-873, 1990.
30. Fawns HT, Landells JW: Histochemical studies of rheumatic conditions. I. Observations on the fine structures of the matrix of normal bone and cartilage. Ann Rheum Dis 12:105-113, 1953.
31. Chen R, Chen S, Chen XM, et al: Study of the tidemark in human mandibular condylar cartilage. Arch Oral Biol 56:1390-1397, 2011.
32. Havelka S, Horn V, Spohrova D, et al: The calcified-noncalcified cartilage interface: the tidemark. Acta Biol Hung 35:271-279, 1984.
33. Stockwell RA: Chondrocytes. J Clin Pathol Suppl (R Coll Pathol) 12:7-13, 1978.
34. Poole CA: Articular cartilage chondrons: form, function and failure. J Anat 191 (Pt 1):1-13, 1997.
35. Wilusz RE, Sanchez-Adams J, Guilak F: The structure and function of the pericellular matrix of articular cartilage. Matrix Biol 39:25-32, 2014.
36. Poole CA, Ayad S, Schofield JR: Chondrons from articular cartilage: I. Immunolocalization of type VI collagen in the pericellular capsule of isolated canine tibial chondrons. J Cell Sci 90 (Pt 4):635-643, 1988.
37. SundarRaj N, Fite D, Ledbetter S, et al: Perlecan is a component of cartilage matrix and promotes chondrocyte attachment. J Cell Sci 108 (Pt 7):2663-2672, 1995.
38. R.A.Stockwell GMa: The Matrix, in M.A.R.Freeman (ed): Adult Articular Cartilage, Vol Pitman Medical Publishing Co Ltd, 1979, pp 33-34.

39. Youn I, Choi JB, Cao L, et al: Zonal variations in the three-dimensional morphology of the chondron measured in situ using confocal microscopy. Osteoarthritis Cartilage 14:889-897, 2006.
40. Lane LB, Villacin A, Bullough PG: The vascularity and remodelling of subchondrial bone and calcified cartilage in adult human femoral and humeral heads. An age- and stress-related phenomenon. J Bone Joint Surg Br 59:272-278, 1977.
41. Newman AP: Articular cartilage repair. Am J Sports Med 26:309-324, 1998.
42. Morales TI: Chondrocyte moves: clever strategies? Osteoarthritis Cartilage 15:861-871, 2007.
43. Lee GM, Loeser RF: Cell surface receptors transmit sufficient force to bend collagen fibrils. Exp Cell Res 248:294-305, 1999.
44. McGlashan SR, Jensen CG, Poole CA: Localization of extracellular matrix receptors on the chondrocyte primary cilium. J Histochem Cytochem 54:1005-1014, 2006.
45. Hoemann CD, Lafantaisie-Favreau CH, Lascau-Coman V, et al: The cartilage-bone interface. J Knee Surg 25:85-97, 2012.
46. Kim IS, Otto F, Zabel B, et al: Regulation of chondrocyte differentiation by Cbfa1. Mech Dev 80:159-170, 1999.
47. van der Kraan PM, van den Berg WB: Chondrocyte hypertrophy and osteoarthritis: role in initiation and progression of cartilage degeneration? Osteoarthritis Cartilage 20:223-232, 2012.
48. Haycock JW: 3D cell culture: a review of current approaches and techniques. Methods Mol Biol 695:1-15, 2011.
49. Buckwalter JA, Martin J, Mankin HJ: Synovial joint degeneration and the syndrome of osteoarthritis. Instr Course Lect 49:481-489, 2000.
50. AL S: Pathology of Osteoarthritis, in Osteoarthritic disorders, Vol. Rosemont, IL, American Academy of Orthopaedic surgeons, 1995, pp 95-101.
51. Neogi T: The epidemiology and impact of pain in osteoarthritis. Osteoarthritis Cartilage 21:1145-1153, 2013.
52. Radin EL, Rose RM: Role of subchondral bone in the initiation and progression of cartilage damage. Clin Orthop Relat Res:34-40, 1986.
53. Ehrlich MG, Armstrong AL, Treadwell BV, et al: The role of proteases in the pathogenesis of osteoarthritis. J Rheumatol 14 Spec No:30-32, 1987.
54. Lotz MK, Otsuki S, Grogan SP, et al: Cartilage cell clusters. Arthritis Rheum 62:2206-2218, 2010.
55. Hoshiyama Y, Otsuki S, Oda S, et al: Chondrocyte clusters adjacent to sites of cartilage degeneration have characteristics of progenitor cells. J Orthop Res 33:548-555, 2015.
56. Buckwalter JA: Mechanical Injuries of Articular Cartilage. Iowa Orthopaedic Journal 12:50-57, 1992.
57. Sidler M, Fouche N, Meth I, et al: Transcutaneous treatment with vetdrop((R)) sustains the adjacent cartilage in a microfracturing joint defect model in sheep. Open Orthop J 7:57-66, 2013.
58. Rietschel ET, Brade H: Bacterial endotoxins. Sci Am 267:54-61, 1992.
59. Nikaido H, Vaara M: Molecular basis of bacterial outer membrane permeability. Microbiol Rev 49:1-32, 1985.

60. Jiang D, Yang Y, Li D: Lipopolysaccharide induced vascular smooth muscle cells proliferation: A new potential therapeutic target for proliferative vascular diseases. Cell Prolif 50, 2017.
61. Goodier MR, Londei M: Lipopolysaccharide stimulates the proliferation of human CD56+CD3- NK cells: a regulatory role of monocytes and IL-10. J Immunol 165:139-147, 2000.
62. Segura MM, Kamen AA, Garnier A: Overview of current scalable methods for purification of viral vectors. Methods Mol Biol 737:89-116, 2011.
63. Mezzina M, Merten OW: Adeno-associated viruses. Methods Mol Biol 737:211-234, 2011.
64. Durand S, Cimarelli A: The inside out of lentiviral vectors. Viruses 3:132-159, 2011.
65. Coffin JM: Retroviruses, in Coffin JM, Hughes SH, Varmus HE (eds): Retroviruses, Vol. Cold Spring Harbor (NY), Cold Spring Harbor Laboratory Press, 1997.
66. Osten P, Grinevich V, Cetin A: Viral vectors: a wide range of choices and high levels of service. Handb Exp Pharmacol:177-202, 2007.
67. Giry-Laterriere M, Verhoeyen E, Salmon P: Lentiviral vectors. Methods Mol Biol 737:183-209, 2011.
68. Miyoshi H, Blomer U, Takahashi M, et al: Development of a self-inactivating lentivirus vector. J Virol 72:8150-8157, 1998.
69. Schawaroch V, Li SC: Testing mounting media to eliminate background noise in confocal microscope 3-D images of insect genitalia. Scanning 29:177-184, 2007.
70. Gantenbein-Ritter B, Sprecher CM, Chan S, et al: Confocal imaging protocols for live/dead staining in three-dimensional carriers. Methods Mol Biol 740:127-140, 2011.
71. Lukinavicius G, Reymond L, D'Este E, et al: Fluorogenic probes for live-cell imaging of the cytoskeleton. Nat Methods 11:731-733, 2014.

7 List of Abbreviations

CLSM	Confocal Laser Microscope
HBSS	Hank`s Balanced Salt Solution
PBS	Phosphate-Buffered Saline
FBS	Fetal Bovine Serum
OATS	Osteochondral Autograft Transfer System
DMEM	Dulbecco`s Modified Eagle Medium
LPS	Lipopolysaccharides from Escherichia coli
TNF α	Tumor Necrosis Factor α
IL1ß	Interleukin-1-ß
GFP	Green Fluorescence Protein
PCV	Packed Cell Volume
MCH	Mean Corpuscular Hemoglobin
MCHC	Mean Copuscular Hemoglobin Volume
MCV	Mean Copuscular Volume
RBC	Red Blood Cells
WBC	White Blood Cells
GOT/ASAT	Glutamyl Oxaloacetic Transaminase / Aspartate Amino Transferase
GGT	Gamma-Glutamyltranspeptidase
CK	Creatine Kinase
Na	Sodium
K	Potassium
Cl	Chloride
Ca	Calcium
Mg	Magnesium
3D	Three-dimensional

Acknowledgement

"When you practice gratefulness, there is a sense of respect towards others."
–Dalai Lama-

Firstly, I would like to express my sincere gratitude to my boss and advisor **Prof. Dr. Brigitte von Rechenberg**.
Brigitte, thank you so much for the continuous support of my thesis and related research, but also your support in all other situations, your patience, motivation, and immense knowledge. It has been very inspiring to meet you.
Also, I want to especially thank **Dr. Salim Elias Darwiche** for his guidance and incredible support! Salim, you helped me in all the time of research and writing of this thesis. I could not have imagined having a better advisor and mentor for my study. Thanks for everything, your friendship, the Israeli-Lebanese-cooking-sessions, the great humor and all the fun times! **IT WAS AN HONOR**!
Thanks to my dear friend **Dr. Sophie Renate Schöberl**, for her support in good and bad times, for crying and laughing with me and understanding me. To many more incredible joined journeys of our life!
Thanks to **Dr. Dagmar Verdino, Dr. Philipp Kindt, Dr. Florian Hipp**, **Dr. Andreas Gloger (alias Wüli) and** soon-to-be-Dr. **David Michalik** for absolutely everything, for being true wonderful friends, and always backing me up when I needed it. Thank you for making my stay in Switzerland unforgettable and for helping me drown my worries and stress in fabulous beer, gin-tonic and Scotch! Thanks for believing in me, supporting me, being reliable in all situations and being absolutely **FANTASTIC FRIENDS**!
Also, I would like to thank my colleagues **Dr. Larissa Arendt**, **Vanessa Graf**, **Marie-Theres Schlote**, **Martina Heygen** and **Alina Steigerwald** for great support, teamwork and friendship!
Special thanks to **Boaz Abraham**, for always lending me an ear, for driving me nuts at work, for singing lovely capoeira songs when I had no chance to flee, for watching Game of thrones with me, teaching me Hebrew and for being my friend, **תודה רבה** !!
Thanks **Dr. Karina Klein** and **Dr. Peter Kronen** for loads of fun at work, for making me want to use headphones during every conversation with you two and especially thank you Karina, for your help and support!

Thank you **Aymone Lenisa** for your histology-input, your great work and help!
Thanks, **Txema** (José Maria Mateos, ZMB, University of Zurich, Switzerland) for your immense help with the confocal microscope! Thanks, **Reto Mair** (Physics Institute, Vetsuisse Faculty Zurich, Switzerland) for your time, ideas and realizations of my rough sketches.
I would also like to thank the rest of the team at the MSRU, **Dr. Katja Nuss**, **Dr. Sabine Koch**, **Rosita Walter**, **Käthi Kämpf**, **Silvana Resegatti** and **Ljubica Dimbrek**, it was great working and spending time with you!
Thanks to **Urs Möri** for being my hero at the "Steri" and helping me with all my crazy instruments.
Without the **Hans-Jörg-Wyss-Foundation** none of this would have been possible! Thanks for sponsoring me!

To my dearest family, **Mom**, **Daddy**, **Shoshana** and my best friend **Denis Klein**, as well as my friends **Anna-Lena Wetzel** and **Benny Giehl** - without your support and especially your faith in me, I wouldn't be where I am now. Thank you so much.

Last but for sure not least, thank you to all the **sheep** that left their lives in the name of research and thank you **Paul Müller** for your respectful interaction with these lovely animals.

Curriculum Vitae

Name	**Serah Naomi Saitowitz**
Birthdate	22.02.1986
Birthplace	Weinheim an der Bergstraße, Germany
Parents	Brian Saitowitz (*25.05.1955 Johannesburg, South Africa)
	Beate Saitowitz (*02.11.1955 Mörlenbach i. Odenwald, Germany)
Nationality	German, Canadian and Israeli
Hometown	Mörlenbach im Odenwald, Germany
1990-1994	Schlosshof-Primary School, Mörlenbach i. Odw., Germany
1994-2005	Liebfrauen-Gymnasium, Bensheim, Germany
2005-2006	Martin-Luther-Gymnasium, Rimbach, Germany, Abitur
24.06.2006	Abitur, Martin-Luther-Gymnasium, Rimbach, Germany
2006-2007	Institute f. Biology & Medicine, Cologne, Germany
2007-2009	Szént Istvàn University, Budapest, Hungary, cand.vet.med.
2010-2015	Freie Universität, Berlin, Germany, vet.med.
25.02.2015	Veterinary medicine degree examination,
	Freie Universität, Berlin, Germany
2015-2018	Preparation of the thesis
	under direction of Prof. Dr. Brigitte von Rechenberg
	at the Musculoskeletal Research Unit, Departement für Pferde
	of the Vetsuisse Faculty University of Zurich
	Director Prof. Dr. Anton Fürst
2017-2018	Internship, Pferdeklinik Salzhofen, Bretten, Germany
2018-today	Equine Veterinarian, Pferdeklinik Salzhofen, Bretten, Germany